JGR Planets

RESEARCH ARTICLE
10.1029/2023JE008155

Special Section:
The Perseverance Rover's Exploration of the Western Fan Front, Jezero Crater, Mars

Depositional and Diagenetic Sulfates of Hogwallow Flats and Yori Pass, Jezero Crater: Evaluating Preservation Potential of Environmental Indicators and Possible Biosignatures From Past Martian Surface Waters and Groundwaters

Kathleen C. Benison[1], Karena K. Gill[1,2], Sunanda Sharma[3], Sandra Siljeström[4], Mike Zawaski[5], Tanja Bosak[6], Adrian Broz[7], Benton C. Clark[8], Edward Cloutis[9], Andrew D. Czaja[10], David Flannery[11], Teresa Fornaro[12], Felipe Gómez[13], Kevin Hand[3], Chris D. K. Herd[14], Jeffrey R. Johnson[15], Juan Manuel Madariaga[16], Morten B. Madsen[17], Jesús Martinez-Frías[18], Marion Nachon[5], Jorge I. Núñez[15], David A. K. Pedersen[19], Nicholas Randazzo[14], David L. Shuster[20], Justin Simon[21], Andrew Steele[22], Christian Tate[23], Allan Treiman[24], Kyle Uckert[3], Amy J. Williams[25], and Anastasia Yanchilina[3]

[1]Department of Geology and Geography, West Virginia University, Morgantown, WV, USA, [2]Now at Department of Earth and Environmental Sciences, Washington and Lee University, Lexington, VA, USA, [3]Jet Propulsion Laboratory, California Institute of Technology, Pasadena, CA, USA, [4]RISE Research Institutes of Sweden, Stockholm, Sweden, [5]Department of Geology and Geophysics, Texas A & M University, College Station, TX, USA, [6]Department of Earth, Atmospheric, and Planetary Sciences, Massachusetts Institute of Technology, Cambridge, MA, USA, [7]Department of Earth Sciences, University of Oregon, Eugene, OR, USA, [8]Space Science Institute, Boulder, CO, USA, [9]Department of Geography, University of Winnipeg, Winnipeg, MB, Canada, [10]Department of Geology, University of Cincinnati, Cincinnati, OH, USA, [11]School of Earth and Atmospheric Sciences, Queensland University of Technology, Brisbane, QLD, Australia, [12]INAF-Astrophysical Observatory of Arcetri, Florence, Italy, [13]Centro de Astrobiologia—CAB (INTA-CSIC), Madrid, Spain, [14]Department of Earth and Atmospheric Sciences, University of Alberta, Edmonton, AB, Canada, [15]Johns Hopkins University Applied Physics Laboratory (JHU/APL), Laurel, MD, USA, [16]Department of Analytical Chemistry, University of the Basque Country UPV/EHU, Leioa, Spain, [17]Niels Bohr Institute, University of Copenhagen, Copenhagen, Denmark, [18]Institute of Geosciences (CSIC-UCM), Madrid, Spain, [19]Department of Space Research and Technology, Technical University of Denmark, Kongens Lyngby, Denmark, [20]Department of Earth and Planetary Science, University of California, Berkeley, CA, USA, [21]NASA Johnson Space Center, Houston, TX, USA, [22]Carnegie Institute for Science, Washington, DC, USA, [23]Department of Astronomy, Cornell University, Ithaca, NY, USA, [24]Lunar and Planetary Institute, Houston, TX, USA, [25]Department of Geological Sciences, University of Florida, Gainesville, FL, USA

Key Points:

- We describe sub-mm scale observations for abrasion patches Berry Hollow and Uganik Island at Hogwallow Flats and Yori Pass on the western fan front in Jezero crater
- These are sulfate-rich clastic rocks with various diagenetic features that suggest sulfate-rich surface waters and groundwater
- Environmental data, such as parent water temperatures and compositions, and any potential biosignatures, may have been preserved

Correspondence to:
K. C. Benison,
kathleen.benison@mail.wvu.edu

Citation:
Benison, K. C., Gill, K. K., Sharma, S., Siljeström, S., Zawaski, M., Bosak, T., et al. (2024). Depositional and diagenetic sulfates of Hogwallow Flats and Yori Pass, Jezero crater: Evaluating preservation potential of environmental indicators and possible biosignatures from past Martian surface waters and groundwaters. *Journal of Geophysical Research: Planets*, *129*, e2023JE008155. https://doi.org/10.1029/2023JE008155

Received 19 OCT 2023
Accepted 18 JAN 2024

Author Contributions:
Conceptualization: Kathleen C. Benison
Formal analysis: Kathleen C. Benison, Karena K. Gill, Benton C. Clark
Funding acquisition: Kathleen C. Benison

Abstract

The Mars 2020 Perseverance rover has examined and sampled sulfate-rich clastic rocks from the Hogwallow Flats member at Hawksbill Gap and the Yori Pass member at Cape Nukshak. Both strata are located on the Jezero crater western fan front, are lithologically and stratigraphically similar, and have been assigned to the Shenandoah formation. In situ analyses demonstrate that these are fine-grained sandstones composed of phyllosilicates, hematite, Ca-sulfates, Fe-Mg-sulfates, ferric sulfates, and possibly chloride salts. Sulfate minerals are found both as depositional grains and diagenetic features, including intergranular cement and vein- and vug-cements. Here, we describe the possibility of various sulfate phases to preserve potential biosignatures and the record of paleoenvironmental conditions in fluid and solid inclusions, based on findings from analog sulfate-rich rocks on Earth. The samples collected from these outcrops, Hazeltop and Bearwallow from Hogwallow Flats, and Kukaklek from Yori Pass, should be examined for such potential biosignatures and environmental indicators upon return to Earth.

Plain Language Summary

Images and compositional data of Mars rocks taken by the Mars 2020 Perseverance Rover at Hogwallow Flats and Yori Pass in Jezero crater show an abundance of sulfate minerals. The goal of this study was to describe the characteristics of these rocks with close-up views of places where these rocks were abraded to expose fresh rock surface, and to make preliminary interpretations of any preservation potential of any possible environmental and biosignature data. We found sand and silt grains with a variety of colors, some of which are sulfate minerals. We also found sulfate mineral crystals between and cross-cutting the grains. The sulfate sand and silt grains may have originally grown as chemical sediments in past salty lakes, and the sulfate crystals found between and cross-cutting the grains formed from past salty groundwater. Sulfate mineral grains and crystals on Earth contain fluid and solid inclusions, which are remnant water, air and other gases, other minerals, and microorganisms and organic compounds. From this knowledge

Investigation: Kathleen C. Benison, Karena K. Gill, Sunanda Sharma, Sandra Siljeström, Adrian Broz, Benton C. Clark, Edward Cloutis, Andrew D. Czaja, Teresa Fornaro, Felipe Gómez, Kevin Hand, Chris D. K. Herd, Juan Manuel Madariaga, Morten B. Madsen, Jesús Martinez-Frías, Marion Nachon, Jorge I. Núñez, David A. K. Pedersen, Nicholas Randazzo, David L. Shuster, Justin Simon, Andrew Steele, Christian Tate, Allan Treiman, Kyle Uckert, Amy J. Williams
Methodology: Kathleen C. Benison, Sunanda Sharma, Sandra Siljeström, Mike Zawaski, Tanja Bosak, Adrian Broz, Andrew D. Czaja, David Flannery, Teresa Fornaro, Felipe Gómez, Kevin Hand, Chris D. K. Herd, Jeffrey R. Johnson, Juan Manuel Madariaga, Jesús Martinez-Frías, Marion Nachon, Jorge I. Núñez, David A. K. Pedersen, Nicholas Randazzo, David L. Shuster, Justin Simon, Andrew Steele, Christian Tate, Allan Treiman, Kyle Uckert, Amy J. Williams
Resources: Sunanda Sharma, Sandra Siljeström, Mike Zawaski, Edward Cloutis, Christian Tate, Kyle Uckert
Visualization: Kathleen C. Benison, Mike Zawaski
Writing – original draft: Kathleen C. Benison
Writing – review & editing: Kathleen C. Benison, Karena K. Gill, Sunanda Sharma, Sandra Siljeström, Mike Zawaski, Tanja Bosak, Adrian Broz, Benton C. Clark, Edward Cloutis, Andrew D. Czaja, David Flannery, Teresa Fornaro, Felipe Gómez, Kevin Hand, Chris D. K. Herd, Jeffrey R. Johnson, Juan Manuel Madariaga, Morten B. Madsen, Jesús Martinez-Frías, Marion Nachon, Jorge I. Núñez, David A. K. Pedersen, Nicholas Randazzo, David L. Shuster, Justin Simon, Andrew Steele, Christian Tate, Allan Treiman, Kyle Uckert, Amy J. Williams, Anastasia Yanchilina

of terrestrial sulfate minerals, we suggest that samples of Hogwallow Flats and Yori Pass, if returned to Earth, should be investigated for fluid and solid inclusions to be evaluated for any enclosed past Martian water, gas, minerals, and possible biosignatures.

1. Introduction

As part of the Mars 2020 mission, the Perseverance rover has examined and sampled rocks, to date and in chronological order, from the Jezero crater floor, the sloped western fan front, the low-relief western fan top, and the crater margin. The key science objectives of this mission include (a) characterizing past habitable environments on Mars; (b) adding to our understanding of the geological and climate history of Mars; (c) caching samples to be returned to Earth for future analyses, including the search for potential biosignatures; and (d) preparing for human exploration of Mars (Farley et al., 2020; Mustard et al., 2013; Williford et al., 2018).

Rock samples are collected by the Perseverance rover using a rotary percussive Coring Drill (Moeller et al., 2021). This system drills and extract cores that are cylindrical in shape, 13 mm in diameter, and up to 78 mm long. Prior to drilling to acquire a rock core, an abrasion patch is made centimeters from the coring target by an Abrading Bit on the rover drill to expose flat, unweathered rock below weathering rinds (Moeller et al., 2021). The abrasion patch is a circular area, 5 cm in diameter and 5–10 mm deep. The fresh rock of the abrasion patch is then analyzed in situ by scientific instruments on the rover. The Standardized Observation Protocol, a systematic set of instrument activities on the abrasion patch and outcrop surface, has been designed for analyses prior to drilling core samples to characterize the outcrop visually and chemically (Bosak et al., 2024; Simon et al., 2023).

During its second Earth year of exploration, the Perseverance rover examined the Hogwallow Flats member at Hawksbill Gap and the Yori Pass member at Cape Nukshak, two strata on the Jezero crater fan front (Figures 1 and 2; Farley & Stack, 2023; Stack et al., 2023). At Hogwallow Flats, two cores named Hazeltop and Bearwallow were collected (Bosak et al., 2024; Herd et al., 2023). A nearby abrasion patch named Berry Hollow was analyzed in situ. At Yori Pass, a core, Kukaklek, was drilled through the abrasion patch Uganik Island. In situ observations based on images and compositional data suggest similar lithologies for these sulfate-rich, fine-grained clastic sedimentary rocks. Descriptions of samples Hazeltop, Bearwallow, and Kukaklek and in situ analytical results from their outcrops and abrasion patches can be found in Farley and Stack (2023).

The objective of this paper is to describe the sedimentology of the sulfate minerals of Hogwallow Flats and Yori Pass rocks based on petrography and composition of abrasion patches Berry Hollow and Uganik Island. From these data, we develop hypotheses for depositional environments and diagenetic processes and discuss the implications of these hypotheses for habitability and the preservation of potential biosignatures. These hypotheses would be tested by analyses of core samples Hazeltop, Bearwallow, and/or Kukaklek in Earth-based labs after sample return anticipated in the 2030's.

2. Background

2.1. Locations

Hogwallow Flats and Yori Pass are located on the southeastern side of the western fan front of Jezero crater (Figure 1). Hogwallow Flats is a low-relief, polygonally cracked, light-toned outcrop of fine-grained sedimentary rock in the Hawksbill Gap region (Figure 2). Abrasion and sampling was conducted at the Wildcat Ridge outcrop, located at ∼−2,523.5 m elevation (below Mars datum surface). The bedrock at Yori Pass is similar in character to Hogwallow Flats and is located at ∼−2,518 m elevation at an outcrop called Hidden Harbor at Cape Nukshak. Hogwallow Flats and Yori Pass are located approximately 0.46 km from each other (Figure 1). They may be stratigraphically and lithologically equivalent. Figure 3 shows the various names used for locations, stratigraphic units, abrasion patches, and samples used in this study.

2.2. Stratigraphic Context

The Hogwallow Flats and Yori Pass members have been assigned to the Shenandoah formation, newly described by Stack et al. (2023) (Figure 4). At Hawksbill Gap, the formation is found from ∼−2,539 to ∼−2,514 m elevation. At Cape Nukshak, the Shenandoah formation is at ∼−2,527 to ∼2,507 m elevation. The Shenandoah

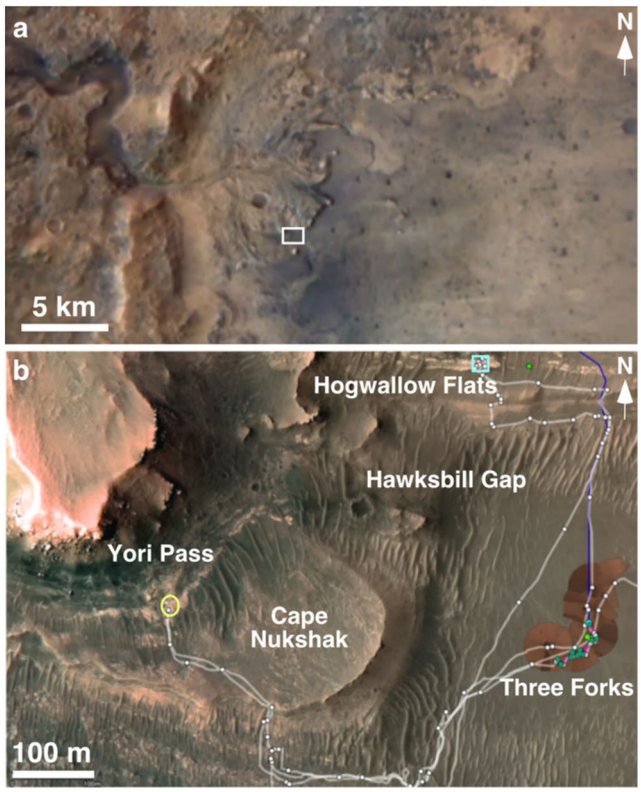

Figure 1. Location of study sites on Mars. (a) Orbital image of western fan in Jezero crater. White box shows the location of image in (b). Image courtesy of ESA/DLR/FU-Berlin. (b) Orbital image of a portion of western fan front investigated by the Perseverance rover, showing locations of sampling of Hogwallow Flats (blue square) and Yori Pass (yellow circle). White line shows traverse by the rover. Image from NASA/JPL-Caltech/University of Arizona/USGS.

formation consists mainly of sandstones and, less commonly, siltstones and granule conglomerates along the western fan front of Jezero crater (Farley & Stack, 2023; Stack et al., 2023; Williams et al., 2023). These clastic sedimentary rocks are characterized by planar laminations, low-angle cross-strata, and possible soft-sediment deformation (Farley & Stack, 2023; Stack et al., 2023; Tebolt et al., 2023; Williams et al., 2023).

Hogwallow Flats and Yori Pass members are found in the middle Shenandoah formation, situated approximately halfway up the thickness of the formation. They are the finest grained rocks in the formation and are characterized by their sulfate veins (Figure 5; Benison, Bosak, et al., 2023; Broz et al., 2023; Nachon et al., 2023). Hogwallow Flats and Yori Pass rocks are each ~3 m thick. These two units seem to be laterally traceable, generally correlative, and lithologically similar. The basal contact for both units appears to be an unconformity or flooding surface. Hogwallow Flats and Yori Pass rocks are underlain by planar laminated sandstones with some soft sediment deformation and lenses of pebbly sandstones. Stratigraphically overlying the Hogwallow Flats and Yori Pass units are cross-stratified sandstones and dipping sand-granule conglomerates (Stack et al., 2023).

2.3. In Situ Investigation

Observations of the Hogwallow Flats and Yori Pass members included imaging and compositional analyses of outcrops, natural surfaces (mainly bedding plane surfaces), and abrasion patches (Figures 6 and 7). This study focuses on observations of the abrasion patch targets Berry Hollow (at Hogwallow Flats) and Uganik Island (at Yori Pass).

Perseverance's onboard instrument suites provide various imaging and chemical data for in situ investigation. The Mastcam-Z's camera system and the SuperCam instrument provide a geologic context for abrasion patches and samples by allowing for imaging and chemical compositional analyses from a distance (i.e., Bell et al., 2021; Maurice et al., 2021; Wiens et al., 2021). Of particular importance to this study, though, are two arm-mounted instruments that can analyze natural outcrop surfaces and abrasion patches at the cm-, mm-, and sub-millimeter scales. The Scanning Habitable Environments with Raman and Luminescence for Organics and Chemicals (SHERLOC), including a Wide-Angle Topographic Sensor for Operations and eNgineering (WATSON), and Planetary Instrument for X-ray Lithochemistry (PIXL) are used at cm standoff distances from rock targets to yield complementary in situ, high-resolution textural and chemical data. SHERLOC, guided by fine-scale imaging, uses Raman and fluorescence spectrometry to detect minerals and organic compounds (Hollis et al., 2023). SHERLOC has an Autofocus Context Imager that is co-boresighted to its spectrometer, and is a fixed focus camera that acquires a 10.1 μm/pixel grayscale image at a nominal 48 mm standoff distance. PIXL uses X-ray fluorescence spectrometry to produce fine-scale elemental compositional data at >120 μm resolution (Allwood et al., 2020).

Hogwallow Flats and Yori Pass rocks are distinct from the underlying and overlying rocks of the western fan front due to their light-toned nature, fine grain size, mottled pink and cream colors, abundance of sulfate minerals, and multiple diagenetic features. Images of outcrops from moderate distances (m–cm scale) show white veins (Figure 5) and spherical, cm-scale concretions. For descriptions of macroscopic diagenetic features, see Broz et al. (2023) and Kulucha et al. (2023). These general preliminary interpretations of Hogwallow Flats and Yori Pass rocks serve to provide a context for this study, which presents observations and hypotheses based on the Berry Hollow and Uganik Island abrasion patches.

2.4. Samples

At the Wildcat Ridge outcrop at Hogwallow Flats, two paired rock samples, Hazeltop and Bearwallow, were cored adjacent to the abrasion patch Berry Hollow (Figure 6). Hazeltop was the 12th sample collected. It was

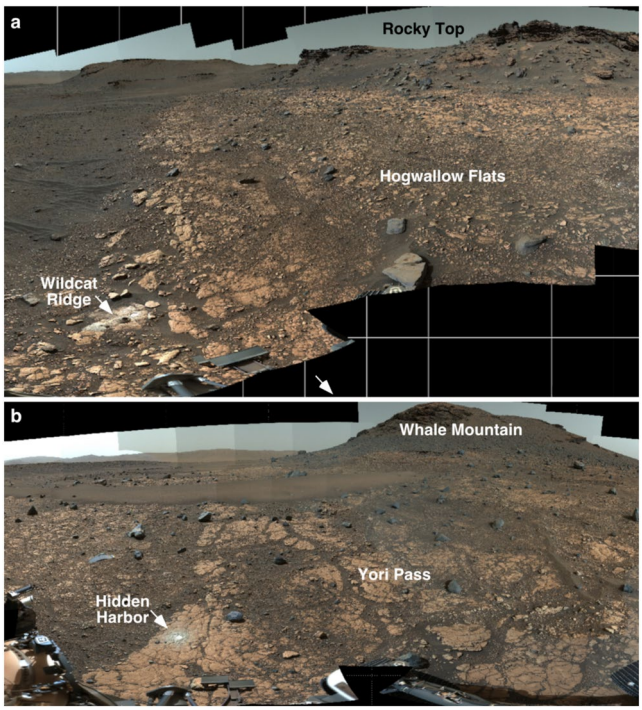

Figure 2. Outcrops at (a) Hogwallow Flats (sol 518; zcam 05842, z04 enhanced color, view to the NW) and (b) Yori Pass (sol 619, zcam 08623, z110 enhanced color, view to the W), as imaged by Mastcam-Z cameras on the Perseverance rover. Credit: NASA/JPL-Caltech/MSSS/ASU. Note white rock powder at abrasion patches and drill holes at Wildcat Ridge and Hidden Harbor outcrops. Wildcat Ridge block is ~0.4 m across and Hidden Harbor outcrop is ~5 m across. For 3D model of Hogwallow Flats, see https://sketchfab.com/3d-models/m2020-zcam-hogwallow-flats-sol-461-b675b747560a4efdbb7369abcac75510. For the 3D model of Yori Pass, see https://sketchfab.com/3d-models/m2020-zcam-hidden-harbor-sol-609-62be9a238f8e4b748359a561c58dd83a.

general location	western fan/delta front, Jezero crater	
formation	middle Shenandoah formation	
region	Cape Nukshak	Hawksbill Gap
member	Yori Pass	Hogwallow Flats
outcrop	Hidden Harbor	Wildcat Ridge
abrasion patch	Uganik Island	Berry Hollow
sample(s)	Kukaklek	Hazeltop Bearwallow

Figure 3. Names of locations, abrasion patches, and samples discussed in this study.

sealed in its titanium tube on sol 509 (27 July 2022; Bosak et al., 2024) and is 5.97 cm long. The 13th sample collected was Bearwallow, sealed in its tube on sol 516 (3 August 2022). Bearwallow is 6.24 cm long. Hazeltop was retained on the Perseverance rover, and Bearwallow was deposited as part of the Three Forks sample cache at the base of the western fan (Figure 1b). At the Hidden Harbor outcrop at Yori Pass, sampling was performed by drilling directly through the Uganik Island abrasion patch to target sulfate diagenetic features there (Figure 7b). The Yori Pass sample, called Kukaklek, was the sixteenth sample collected, was sealed on sol 631 (29 November 2022), and is 4.97 cm long. It was retained on the rover.

3. Methods and Approach

For this study, we focus on the petrography of the abrasion patches Berry Hollow and Uganik Island to describe depositional and diagenetic features at the cm–sub-mm scale. We pay particular attention to the sulfate mineral components of these rocks due to their potential to preserve biosignatures (i.e., Benison, 2019a; Gill et al., 2023; Longo et al., 2019; Martinez-Frias et al., 2006; Sharma et al., 2023). The wider context of depositional history, stratigraphic context, and diagenetic features can be found in other recent papers (i.e., Broz et al., 2023; Dehouck et al., 2023; Farley & Stack, 2023; Kalucha et al., 2023; Stack et al., 2023). Finally, we employ the concepts of comparative sedimentology and cross-cutting relationships to make initial interpretations about depositional environments and diagenetic history, respectively. From these interpretations, we develop hypotheses about the potential for biosignatures and environmental proxies. The results of this study may provide foundational knowledge of Bearwallow, Hazeltop, and Kukaklek samples that can guide the curation and lab studies of these samples upon return to Earth.

Despite the engineering achievements of abrading and imaging (at the sub-mm scale) rock surfaces on another planet, there are some limitations to conducting petrography in situ on Martian rocks. First, the optical resolution does not allow us to resolve objects smaller than ~30 μm; many petrographic microscopes on Earth can detect objects as small as 1 μm. In addition, in situ abraded surfaces on Mars do not allow inspection through an ultrathin (~30 μm), polished surface of the rock with transmitted light, as thin sections would allow. Therefore, petrographic observations of in situ images of abrasion patches on Mars do not allow us to distinguish some individual grain and crystal boundaries, especially at the sub-mm scale. We anticipate that, upon return to Earth, refined petrographic observations would be made of Martian samples in Earth laboratories.

4. Results

4.1. Hogwallow Flats: Berry Hollow Abrasion Patch

4.1.1. Petrography

Visual observations of the Berry Hollow abrasion patch show that it is a clastic sedimentary rock that has grains and diagenetic features (Figure 8). Grains are silt-, very fine sand, and fine sand-sized and the rock appears to be well-sorted. Wentworth (1922) defined silt as grains in the range of 0.0039 mm (3.9 μm) to 0.0625 mm (62.5 μm), very fine sand as grains in the range of 0.0625–0.125 mm, and fine sand as grains in the range of 0.125–0.25 mm. However, the size detection limit of ~30 μm does not allow us to determine whether there are also grains of fine silt size or smaller. Most

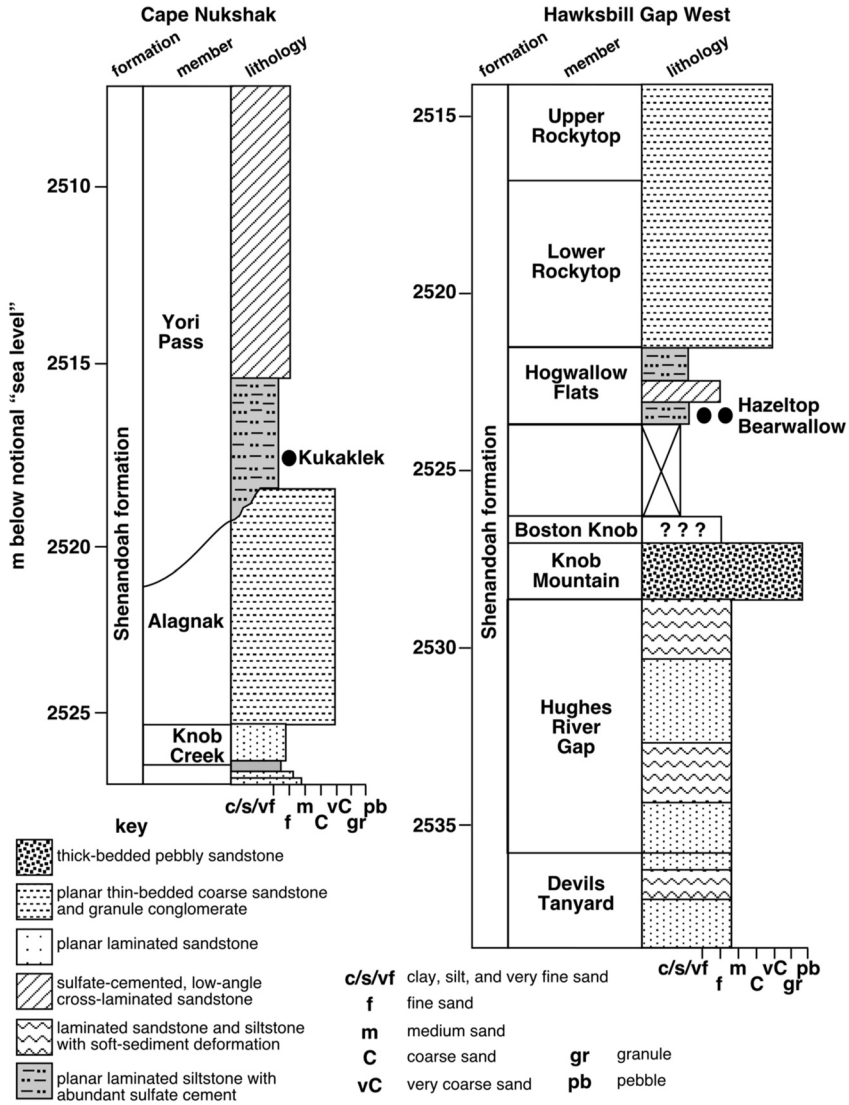

Figure 4. Stratigraphic columns of the Shenandoah formation at Cape Nukshak and the western part of Hawksbill Gap, showing the context of Yori Pass and Hogwallow Flats members. Approximate locations of samples Kukaklek, Hazeltop, and Bearwallow are shown with black dots. The abrasion patch Uganik Island is the same target as Kukaklek. Abrasion patch Berry Hollow was cm from cores Hazeltop and Bearwallow. Modified after Stack et al. (2023).

grains are moderately—highly spherical and moderately—well-rounded, although a small percentage is subangular to angular. There are a range of colors of the grains; some appear black-dark gray, others red-brown, others are cream-colored, and some are white. Overall, the rock has a mottled pink and tan appearance.

Many grains are surrounded by a distinctive cream-colored rim (Figures 8b and 9). Rare pale orange rims surround some cream-colored grains. Some white grains appear not to have a cream-colored or pale orange rim. The rock has an overall mottled appearance, with patches of pink and tan that appear to surround the grains and their cream-colored rings. Tiny (sub-mm-thick) white veinlets are observed.

4.1.2. Elemental and Mineral Composition

In situ analyses of the Berry Hollow abrasion patch indicates that it contains phyllosilicates and Mg-Fe sulfates (likely hydrated), with minor amounts of the anhydrous Ca sulfate anhydrite, hematite, possible carbonates, and possible chloride salts (Bosak et al., 2024; Hurowitz et al., 2023; Núñez et al., 2023; Phua et al., 2023; Roppel et al., 2023). This rock is composed of more than 30% sulfate minerals. The host rock is enriched in Fe-Mg-sulfates and much smaller amounts of Ca- and Fe-sulfates. Chlorine-containing salts contribute less than 1% of the rock

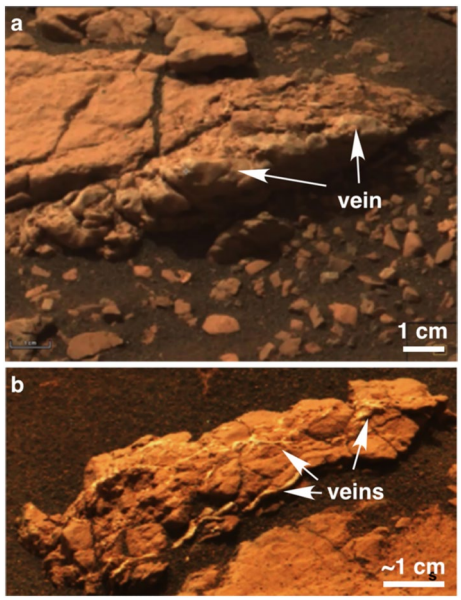

Figure 5. Veins at Hogwallow Flats (Sol 510, zcam0833, cropped images). (a) Approximately 2 cm wide vein. (b) Thin bifurcating veinlets. Credit: NASA/JPL-Caltech/MSSS/ASU.

target volume. The veins are composed primarily of Ca sulfates, including anhydrite confirmed by laser Raman spectroscopy and possibly hydrated Ca sulfates such as gypsum (Lopez-Reyes et al., 2023). There is a patchy pink and tan appearance to the abrasion patch. The pink areas are relatively Si-rich and/or sulfate-poor, compared to the more sulfate-rich tan patches. Ferric sulfates, most likely jarosite ($KFe^{3+}_3(SO_4)_2(OH)_6$) and copiapite ($Fe^{2+}(Fe^{3+})_4(SO_4)_6(OH)_2{\cdot}20H_2O$), were detected in the Berry Hollow abrasion patch as well as in the tailings (Dehouck et al., 2023). Phyllosilicates are likely Fe-smectites, such as nontronite.

4.2. Yori Pass: Uganik Island Abrasion Patch

4.2.1. Petrography

In the Uganik Island abrasion patch, most grains range from very fine sand-sized to medium sand-sized (Figure 10). However, there is also a granule-sized, rounded feature of tan sandstone. Grains are moderately sorted, rounded-angular, and have moderate-high sphericity. As in Berry Hollow, grains exhibit a variety of colors, including black/dark gray, tan, and cream.

Cream-colored rims can be seen on some grains (Figure 10b). Like Berry Hollow, Uganik Island is characterized by pink and tan mottling, although the color differences may be more subdued in Uganik Island than in Berry Hollow. White and cream-colored, mm-scale crystalline veins and patches

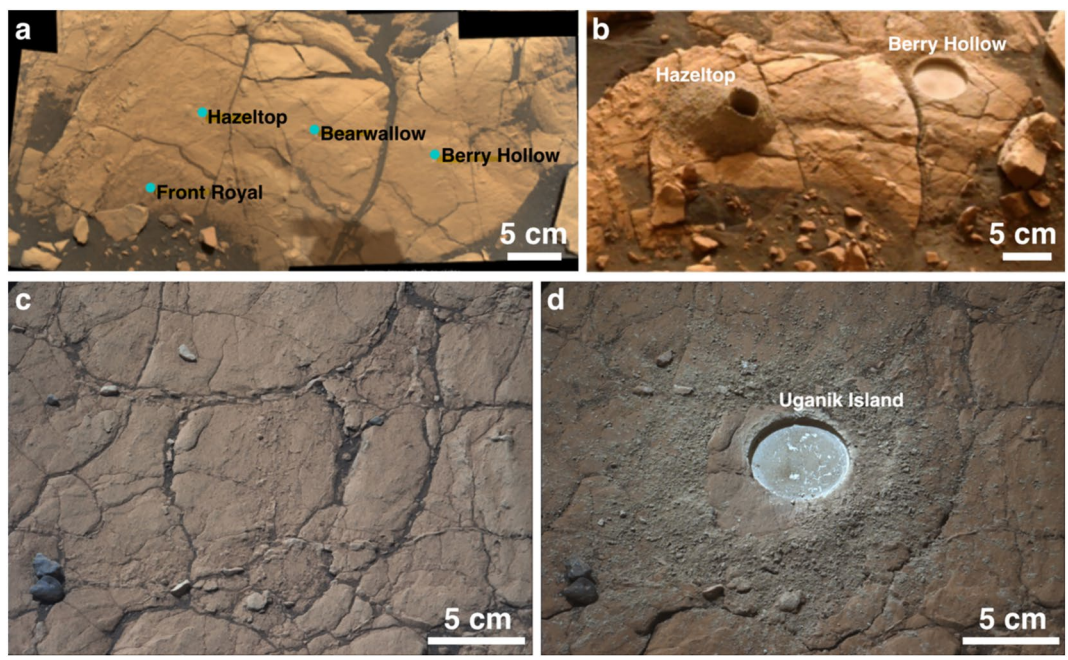

Figure 6. Views of bedding planes at abrasion and sampling sites. (a) and (b) Wildcat Ridge outcrop at Hogwallow Flats: (a) natural surface prior to abrasion and sampling (Sol 503, srlc 04001); (b) abrasion patch Berry Hollow at right; post-sampling borehole and tailings pile of Hazeltop sample site on the left; area between abrasion patch and Hazeltop borehole was drilled to obtain Bearwallow sample (Sol 518, zcam 08541). For a movie showing the time sequence of abrading and drilling, see https://sketchfab.com/3d-models/m2020-zcam-wildcat-ridge-sol-502-518-7cbc03c7bfb344f8ae6cc7a11ba52a1e. (c) and (d) Hidden Harbor at Yori Pass: (c) natural surface prior to abrasion and sampling (Sol 612, zcam 03480); (d) abrasion patch Uganik Island; drilling of sample Kukaklek was done through the abrasion patch to target sulfate veins and vugs (Sol 614, zcam 03487). Credit: NASA/JPL-Caltech/MSSS/ASU. For a movie showing the time sequence of abrading and drilling, see https://sketchfab.com/3d-models/m2020-zcam-wildcat-ridge-sol-502-518-7cbc03c7bfb344f8ae6cc7a11ba52a1e.

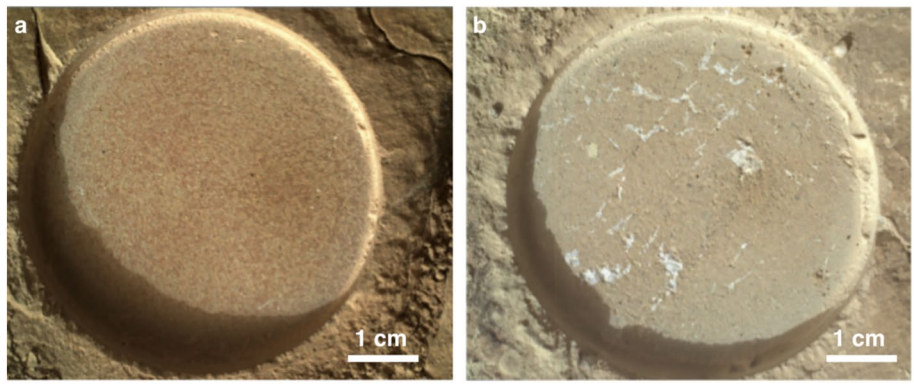

Figure 7. Abrasion patches Berry Hollow (a) at Hogwallow Flats (Sol 504, srlc 02504) and Uganik Island (b) at Yori Pass (Sol 612, srlc 00746).

cross-cut all other features seen in the abrasion patch (Figure 10a; Núñez et al., 2023; Phua et al., 2023; Roppel et al., 2023). Veins on Uganik Island are less than 1–2 mm thick and up to ∼12 mm long; some have 90° angles and branches. Both veins and patches are filled with at least two cement detectable in abrasion patch views at the mm-scale (Figures 10d and 10e). The veins are lined with fine cream-pale yellow crystals and filled with coarser pale gray crystals. The largest white crystalline patch seen in Uganik Island is ∼5 mm across and is roughly "fish"-shaped. The "dorsal fin" on the top side of "fish" shows at least four generations of crystals (Figure 10d). These crystal generations are distinguished by slight color variations including white, cream, and pale gray. Each generation has crystals that point in one direction (appear upward in abrasion patch images; Figure 10d).

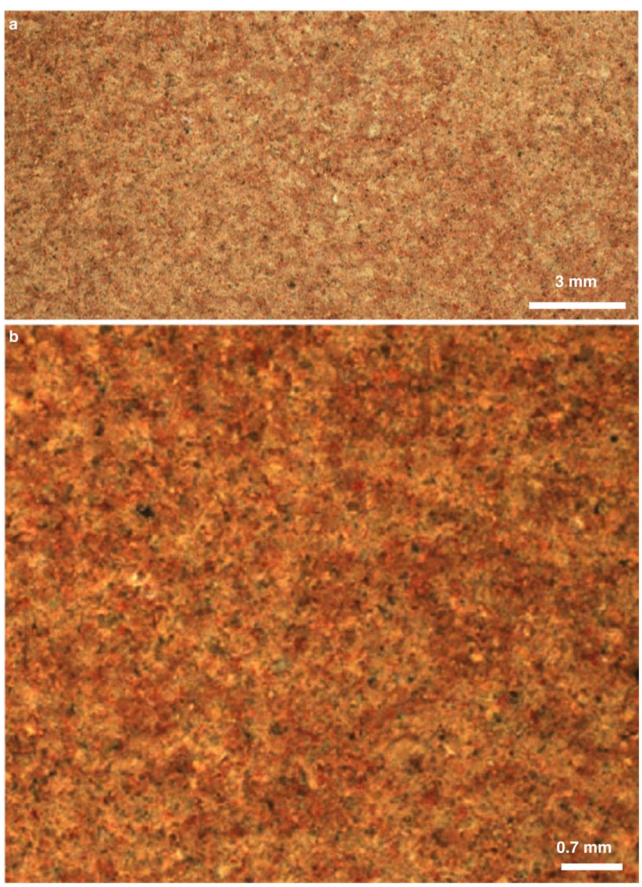

Figure 8. Close-up views of Berry Hollow abrasion patch show textures (Sol 505, srlc 00009 colorized). (a) Pink and cream patches. (b) Relationship of grains to pink and cream patches. Note various grain colors.

4.2.2. Elemental and Mineral Composition

Uganik Island abrasion patch contains phyllosilicates, the anhydrous Ca sulfate anhydrite, hydrated Fe-Mg sulfates, and possible ferric sulfate (Figure 11; Hurowitz et al., 2023; Núñez et al., 2023; Phua et al., 2023; Roppel et al., 2023). Hematite is localized. As with the Berry Hollow abrasion patch, chloride salts may also be present. The white-cream veins and crystal patches have been identified as anhydrite (Hurowitz et al., 2023; Lopez-Reyes et al., 2023; Roppel et al., 2023).

5. Interpretations

5.1. Deposition and Diagenesis of Hogwallow Flats and Yori Pass Members

A schematic overview of observations and interpretations of depositional and diagenetic features in Berry Hollow and Uganik Island is provided in Figure 12. Depositional features are those that formed when the sediment first accumulated at the current location of the rock. Sedimentary textures (including grain size, grain sorting, and grain morphology), grain composition, and sedimentary structures (such as bedding and ripple marks) are depositional characteristics described in sedimentary rocks. Diagenetic features are products of any physical, chemical, or biological processes that may have occurred to the sediment after deposition. Cement, dissolution features, and weathering rinds are all examples of diagenetic features. Our interpretations described below are not intended as a final interpretation of the history of these rocks, but rather as a first interpretation based solely on in situ imaging and compositional data collected by the Perseverance rover. Only further examination of these rocks on Earth will refine the interpretations of their depositional and diagenetic histories.

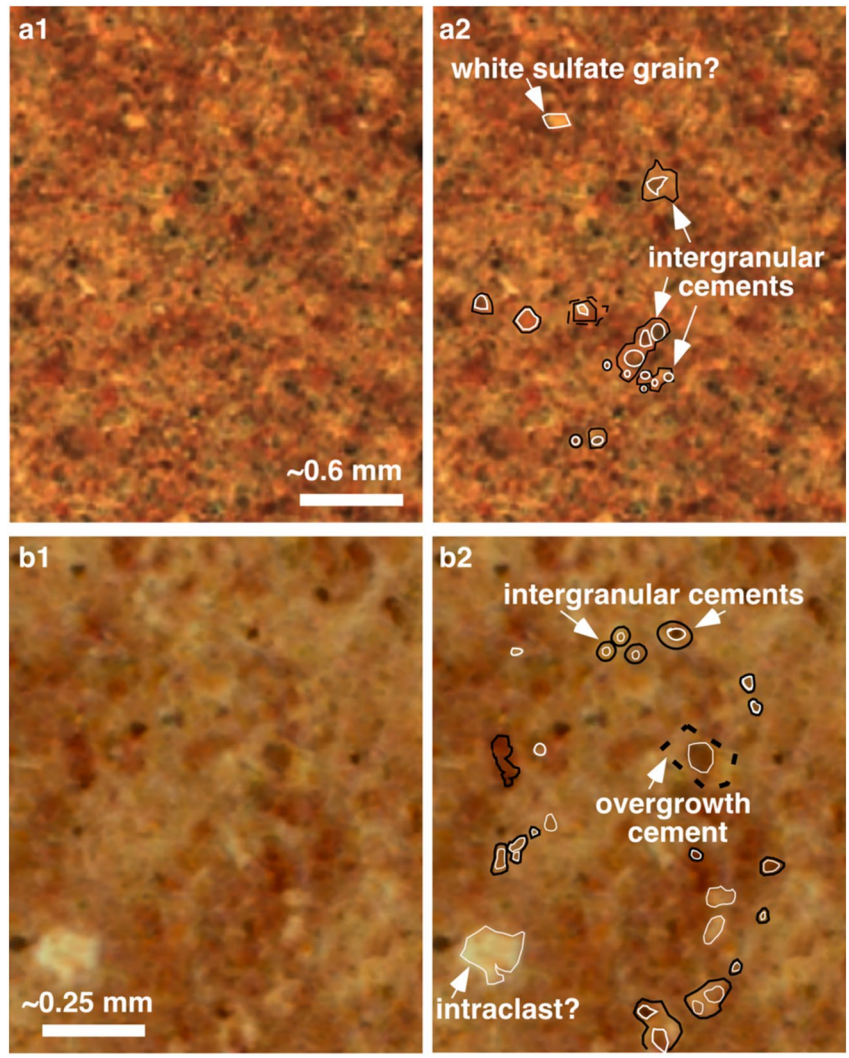

Figure 9. Close-up in situ views of Berry Hollow abrasion patch (a1) and (a2) show textures at highest magnification that retains the focus (Sol 505, srlc 00009, colorized). (b1) and (b2) Closest view before resolution is lost to attempt to image individual grains and cement (Sol 505, srlc 00009, colorized). Images (a2) and (b2) are annotated versions of images (a1) and (b1), respectively. White lines outline select individual grains. Black solid lines highlight intergranular cement. Dashed black lines trace overgrowth cement.

5.1.1. Deposition

Berry Hollow's silt and fine sand grains and Uganik Island's fine to medium sand grains of various colors suggest that these are clastic grains. The grains are likely of various compositions. Cream-colored and white grains are likely composed of different sulfate minerals containing Ca and/or Fe-Mg. Black and gray grains may be phyllosilicate-rich intraclasts. Dark red-brown grains may be hematite grains. Some of the larger clasts in the Uganik Island abrasion patch may be lithic clasts. There are no grains with shapes, sizes, colors, textures, or compositions that appear consistent with terrestrial carbonate grain types. We interpret the grains as physically reworked clasts, sourced from the weathering and erosion of pre-existing rocks. Suspect phyllosilicate grains may have been locally sourced from mud that was cemented early and then eroded and rounded as mud clump clasts. We think it is likely that some of the sulfate grains may have originally been sulfate crystals that became clasts by erosion and reworking by physical processes.

Reworked sulfate clastic grains are known on Earth (i.e., Benison, 2019b; Benison, 2017; Benison & Bowen, 2013; Benison et al., 2016, 2007; Langford, 2003; Mees et al., 2012; Zheng et al., 2003). Sulfate minerals precipitate as crystals from surface or subsurface saline waters. These crystals can later be moved from the location of

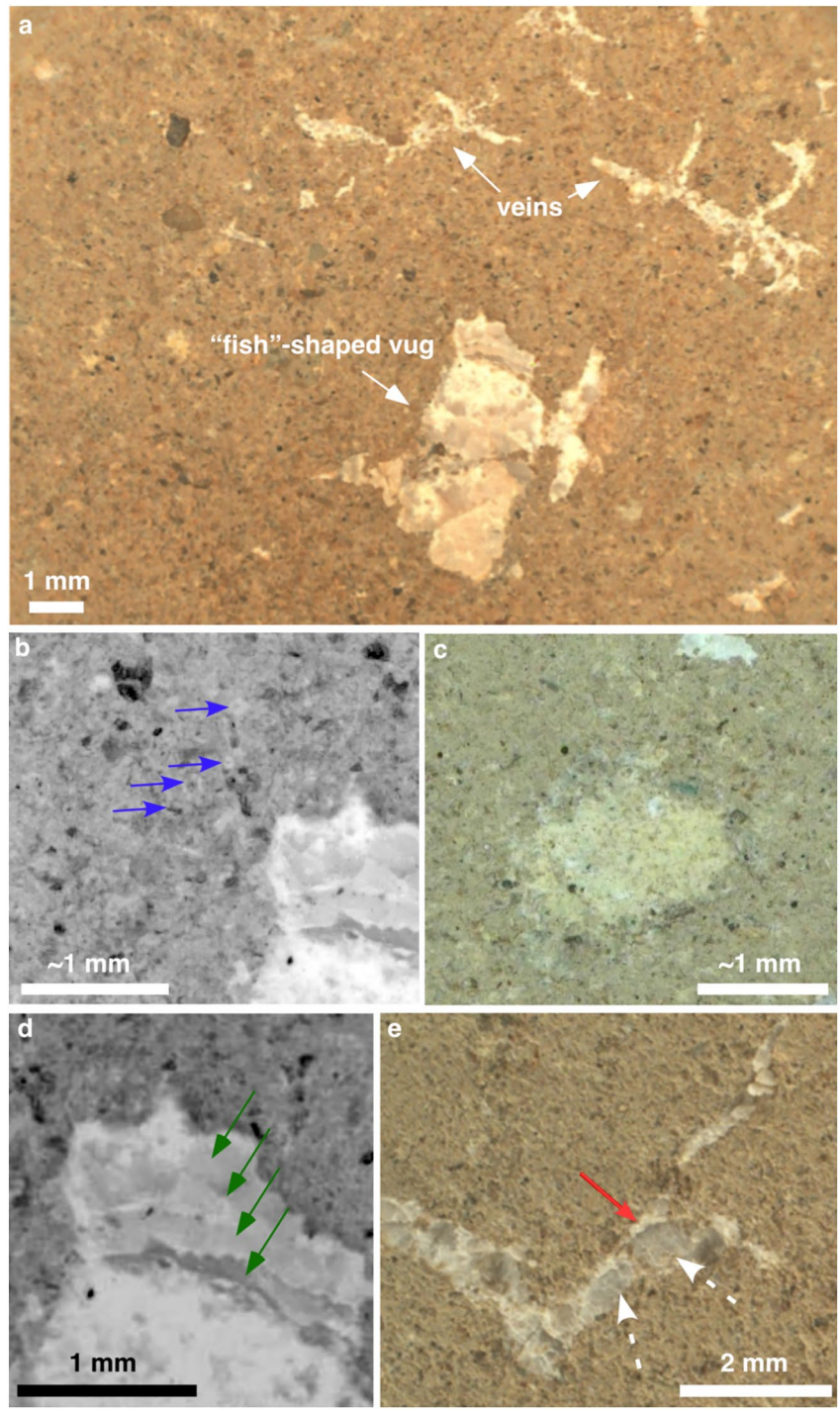

Figure 10. Close-up views of Uganik Island abrasion patch. (a) View of depositional and diagenetic features, including white veins and fish-shaped vug, both filled with Ca-sulfate cement crystals (Sol 614, srlc 00003). (b) Blue arrows point to cream-colored isopachous intergranular cement around sand grains. The large white patch in the lower right are cement crystals in fish-shaped vug (Sol 614, srlc 10600, cropped greyscale image). (c) Patch of localized potential intraclast with yellow intergranular cement (Sol 614, srlc00643, cropped). (d) Close-up view of "dorsal fin" of "fish" crystal patch. Green arrows point to several generations of crystals that point outward (Sol 614, srlc 10600, greyscale image, cropped). (e) Vein with two generations of Ca-sulfate cement; red arrow points to the first generation of cement, lining vein; dashed white arrows point to larger crystals of the second generation of vein-filling cement (Sol 614, srlc 00643, cropped).

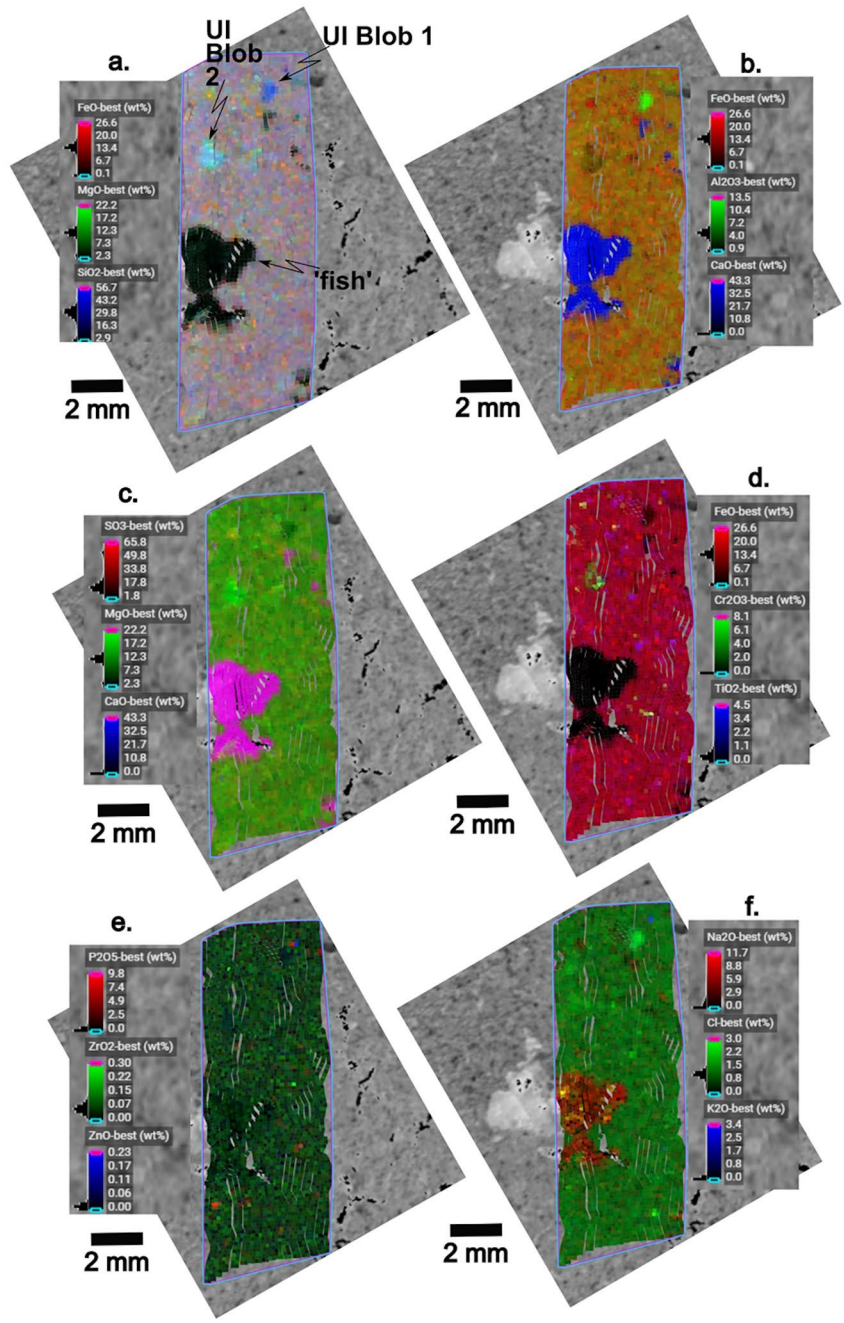

Figure 11. (on preceding page): PIXL compositional maps (Sol 614) of a portion of Uganik Island abrasion patch, showing "fish" vug as a prominent feature, as well as host rock. Note different orientation of "fish"-shaped crystal patch compared to images of it in Figure 10 (a); PIXL data are rotated 90° clockwise. Here, the fish "tail" is pointing down. Panels (b) and (c), respectively, show strong signals for Ca and S signals in this crystal patch. Panel (f) suggests some Na in the "fish." Host rock contains Fe, Mg, Si, S, and Cl, with traces of Zr.

their formation by water, wind, or gravity; during these "reworking" processes, they are broken, smoothed, and undergo a decrease in size. For example, White Sands National Park in New Mexico, USA provides a good example: gypsum crystals grown as bottom-growth crystals in Lake Lucero and displacive gypsum crystals precipitated from shallow saline groundwater are subaerially exposed during lake desiccation and eolian blowout of surface sands, respectively (Benison et al., 2016). Grains are then broken by winds and moved by those winds. Eventually, those broken gypsum crystals become the rounded sub-rectangular and spherical gypsum sand grains

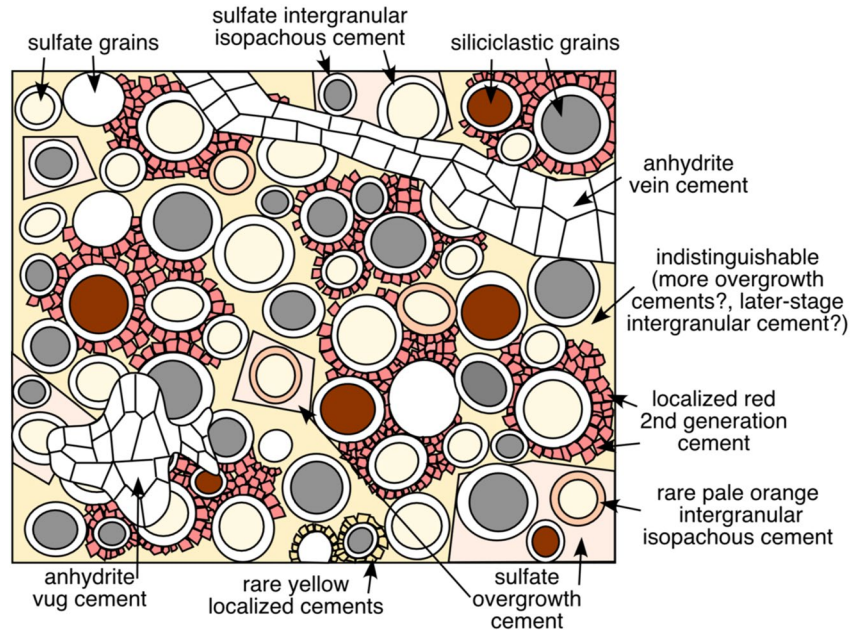

Figure 12. Schematic model depicting preliminary interpretations of silt and sand grains and cement and their petrographic relationships, at mm-cm-scale, of Hogwallow Flats and Yori Pass rocks, based on images of abrasion patches Berry Hollow and Uganik Island. Pink and tan mottling was likely formed by second generation overgrowth cement, localized red intergranular cement, and rare yellow intergranular cement, all of which appear to have formed after cream-colored first-generation intergranular cement and before veins and vugs. Limitations in resolution of smaller grain and crystal sizes, as well as poor focus on some grain and crystal boundaries due to unpolished abrasion, do not allow for the distinction of some of the later cement in the rock. Fluid inclusions and possible biosignatures may potentially be found in sulfate grains and the various sulfate cement.

that comprise the famous White Sands dunes. Gypsum clasts can also be moved by water. In shallow saline lakes in Western Australia and Chile, bottom-growth and cumulate gypsum grains, as well as displacive gypsum crystals, are entrained by winds and flood waters and deposited as reworked grains in their parent lake, in sandflats, mudflats, soils, and dunes near the parent lakes, or can be deposited in a second lake (i.e., Benison et al., 2007; Benison, 2017). At White Sands, the grains are dominated by gypsum. But in Western Australia, the reworked sulfate grains are mixed with siliciclastic grains sourced from weathering of Archean and Proterozoic igneous, metamorphic, and sedimentary rocks (Benison & Bowen, 2013; Benison et al., 2007). These siliciclastic grains include quartz (and other silicates), some of which are hematite-coated. At Salars Gorbea and Ignorado in northern Chile, the water- and wind-reworked grains are either predominantly gypsum or a mixture of gypsum and clasts of local igneous rocks (Benison, 2019b). Therefore, although any sulfate grains in the Hogwallow Flats or Yori Pass rocks were precipitated from saline water, we propose here that they were not necessarily deposited in their parent lake. Parent lakes or groundwater may have been meters to kilometers from the depositional environment (at Hogwallow Flats and Yori Pass) of the sulfate grains.

On Earth, sedimentary geologists use five distinct characteristics of a sediment to characterize it and as clues to interpret depositional processes and environment: (a) sedimentary textures, including grain size, sorting, roundness, sphericity, and any grain surface textures; (b) color and composition; (c) sedimentary structures; (d) fossils; and (e) 3D geometry of deposit. In addition, depositional interpretations of rocks lying conformably below and above the stratigraphic unit of interest can also be helpful in making reasonable depositional interpretations. In contrast, our depositional interpretations of the Hogwallow Flats and Yori Pass members rely mainly on the sedimentary textures, color, and composition. Outcrops of these units exist mainly as bedding planes, and much of those bedding planes are partially covered with regolith, so we see few vertical exposures to evaluate for cross-sectional views of sedimentary structures. The sedimentary structures seen are some planar laminations, low-angle cross-stratification, and possible soft-sediment deformation (Stack et al., 2023).

Based on the sedimentary textures, colors, and compositions of the Berry Hollow abrasion patch and the sedimentary structures seen in adjacent rocks, we cannot make a definitive interpretation of the depositional environment.

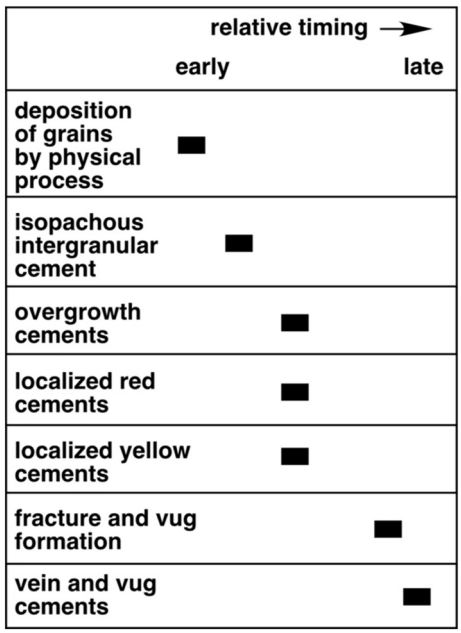

Figure 13. Paragenetic sequence of features based on observations of abrasion patches Berry Hollow and Uganik Island. Other diagenetic features (such as concretions) seen in Hogwallow Flats and Yori Pass outcrops (but not in abrasion patches) are not included here.

Three possible depositional environments include (a) lacustrine; (b) fluvial/delta; or (c) subaerial sand flats on an alluvial fan (where wind and/or floods may have occurred). Well-sorted silts and fine sands, with planar laminations, low-angle cross-stratification, and soft-sediment deformation are all found in some lakes, some rivers and deltas, and some subaerial sand flats on Earth.

5.1.2. Diagenesis

Observations presented here for the Berry Hollow and Uganik Island abrasion patches strongly suggest that there were multiple sulfate-rich and some Fe-rich groundwaters that flowed through these sediments. Cream-colored rims seen around some grains are interpreted as a first-generation isopachous intergranular cement. This cream-colored cement is likely composed of a sulfate mineral due to the color, the abundance of sulfate in the rock, and the tendency for sulfate minerals on Earth to form early cement. Some white grains have no obvious first-generation cream-colored cement. This may be due to the grains having the same composition as the cream cement, so the cement may be there but not visually recognizable. Other white-cream grains have a pale orange rind, which may represent either a first-generation intergranular cement of a different composition than the cream cement, or an alteration rind where other edges of the host sulfate grain were replaced by a different mineral. The pale orange color, with consideration of the detected composition of the rock, suggests that these rinds may be jarosite or hematite, which would indicate the presence of an acidic oxidized sulfate-rich fluid responsible for this early cement.

Second generation diagenetic events include overgrowth cement and localized intergranular cement. The pink and tan mottling may be due to second-generation cement, including tan overgrowth cement, localized patches of hematite cement, and rare patches of yellow cement, consistent with a possible presence of goethite or jarosite for those Fe-rich cement. The localized red cement (and possibly yellow cements) may represent early phases of concretion formation. It is difficult to distinguish timing among these different second-generation features, partly due to their localized nature, the limitations on observations of sub 30 μm grain and crystal sizes, and the unpolished rock surface. Thin section petrography that allows for higher-resolution imaging using transmitted light would allow refinement of these features upon return to Earth. Regardless of the limitations on interpretations of these overgrowths and second-generation intergranular cement, it seems likely that they are responsible for the pink and tan mottling of the rocks.

The veins and vugs are interpreted as late-stage diagenetic features because they appear to cross-cut other diagenetic features of these rocks. Veins seen in the Uganik Island abrasion patch have two cement generations: the pale yellow-cream crystals that appear on the outer edges of veins formed first and the coarser, pale gray crystals on the interior of veins formed last, filling the veins. The “fish”-shaped patch appears as a relatively large feature at first. It is different from the veins in both its morphology and the crystal generations. The “fish”-shaped crystal patch appears to either be a vug (a randomly shaped dissolution feature smaller than a cave) filled with cement crystals or a relatively large vein that does not look elongated due to the cross-sectional cut of the abrasion surface. However, upon closer inspection, the “dorsal fin” part of the “fish” shows several generations of crystals directed in one direction. This is curious because these crystals point toward the outer edge of the “dorsal fin” crystal patch, yet cement in a pore space grow toward the middle of the open pore. A possible interpretation is that the “fish” is actually two diagenetic features: the main “fish” body is a vug or vein filled with cement, and the “dorsal fin” is a clast of bottom-growth crystals that would have grown in saline surface water (lake) and been eroded and deposited as a clump of crystals with the other grains at Yori Pass.

Our interpretation of the most likely paragenetic sequence is shown in Figure 13. Figure 14 illustrates a depositional and diagenetic model with four main events. The first-generation intergranular isopachous cement likely precipitated relatively early from saline groundwater. The second-generation features, including overgrowth cement and localized red and yellow intergranular cement, formed next. The veins and “fish”-shaped vug formed

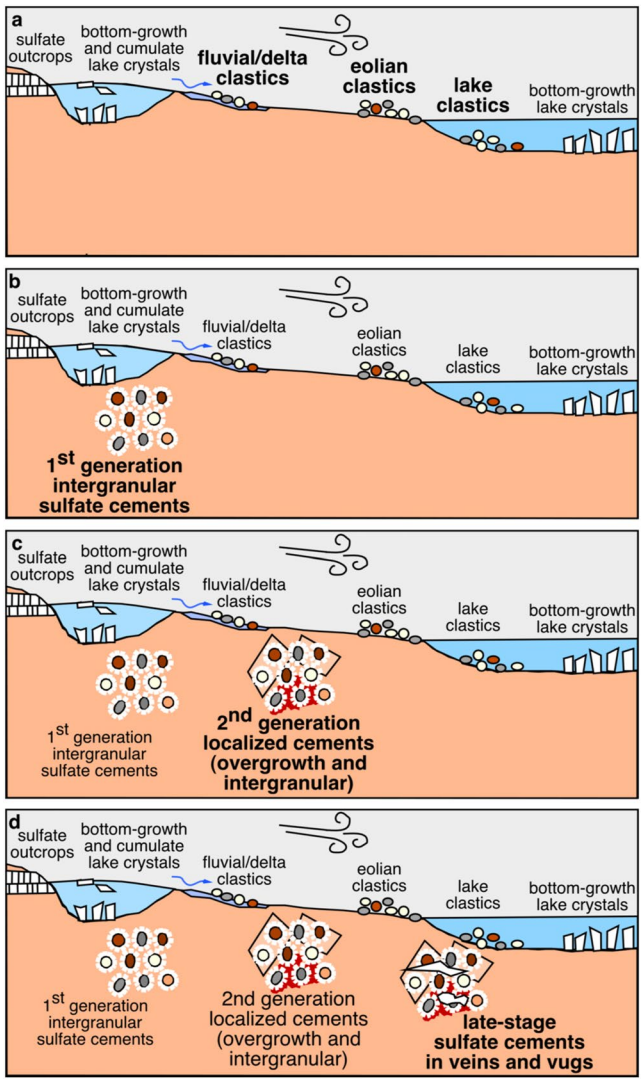

Figure 14. Depositional and diagenetic model for Hogwallow Flats and Yori Pass members, shown through relative time. (a) Deposition of mixed siliciclastics and clastic sulfate grains on Jezero crater western fan front may have been in fluvial/delta, eolian sand flats, or lake setting. Clastic sulfate grains are likely reworked bottom-growth or cumulate crystals from saline lakes or eroded clasts from upstream sulfate rock outcrop. (b) Cream-colored (and less common pale orange) isopachous intergranular cement crystals form rings around grains; they were likely precipitated from an early, shallow saline groundwater. (c) Second generation cement that cause the pink and tan mottling may have precipitated as overgrowth cement and as localized intergranular cement. Localized red cement may be related to the early stages of Fe-oxide concretion formation. Second generation cement likely also formed from saline groundwater. (d) Veins and vugs filled with one or two generations of Ca-sulfate cements are late-stage diagenetic features that cross-cut grains and earlier cement; they also precipitated from saline groundwater.

relatively late. There are no obvious indicators of compaction observed in these rocks.

6. Discussion

6.1. Are There Terrestrial Analogs for the Hogwallow Flats and Yori Pass Rocks?

There are sediments and rocks on Earth that have sulfate grains and sulfate diagenetic features. Relatively few, though, are fine-grained clastic rocks that also contain hematite and phyllosilicates. Good petrographic analogs are Permo-Triassic red beds and evaporites of continental Pangea, now deposits in the midcontinental USA, Brazil, and Northern Ireland, as well as recent acid saline lake-adjacent sandflats/mudflats. For example, the sedimentary sequence in western Kansas (USA) includes the mid-Permian Ninnescah Shale and the Triassic Dockum Group, fine-grained siliciclastic rocks with mottled pink and tan coloration (Figures 15a and 15b; Zambito et al., 2012). Their grains include quartz (some coated in hematite) and reworked gypsum clasts. Both the Ninnescah Shale and Dockum Group have early gypsum, hematite, and phyllosilicate cement, and late-stage gypsum and anhydrite veins. These Permo-Triassic red bed and evaporite deposits formed in shallow perennial and ephemeral acid saline lakes, sandflats/mudflats, ephemeral channels, dunes, and desert soils. Shallow groundwater were acid brines that precipitated halite, gypsum, anhydrite, bassanite, jarosite, alunite, hematite, kaolinite, halloysite, and rare opalline silica just centimeters below the surface. Modern counterparts are acid saline lake systems in Western Australia and hydrothermally influenced acid saline lake systems in northern Chile (Benison, 2019b; Benison et al., 2007). Figure 15c shows a view of a potential Hogwallow Flats/Yori Pass analog from a mudflat adjacent to an acid saline lake in Western Australia. The Permo-Triassic red beds and evaporites host abundant gypsum/anhydrite veins, but the modern sediments do not, supporting the interpretation that the veins are late-stage diagenetic features.

The acid saline lake deposits of modern Western Australia and Chile and the Permo-Triassic of Pangea have been studied for their microbiology. Despite the extreme and complex water chemistry, with pH less than 2 and sometime less than 0, salinity up to 10× seawater concentration, abundance of dissolved metals, and low water activity measurements (as low as 0.714 for modern lakes in Western Australia; Benison et al., 2021), these environments are/were habitable. Microbial surveys in modern acid salt lakes and groundwater have documented diverse microbiological communities; many of these microorganisms are novel (i.e., Benison, Bosak, et al., 2023; Benison, Hallsworth, et al., 2023; Davis-Belmar et al., 2013; Escudero et al., 2018; Johnson et al., 2015; Mormile et al., 2009; Zaikova et al., 2018). Modern halite and sulfate crystals precipitating from these acid brines contain microorganisms and organic compounds (i.e., Benison, 2013, 2019a; Benison & Karmanocky, 2014; Benison, Bosak, et al., 2023; Benison, Hallsworth, et al., 2023; Conner & Benison, 2013). Ancient acid brine salt minerals, including halite from the Proterozoic Browne Formation of Australia, the Permo-Triassic Nippewalla Group of Kansas and Oklahoma, and the Opeche Shale of North Dakota, and unaltered gypsum from the Chugwater Group of Wyoming, contain microorganisms and organic compounds in primary fluid inclusions and as solid inclusions (i.e., Schreder-Gomes et al., 2022).

Although some of the microorganisms, including cells of archaea, bacteria, algae, and fungi preserved in ancient halite, are extremophiles that lived in the acid saline lakes, other microorganisms, including some common fungi,

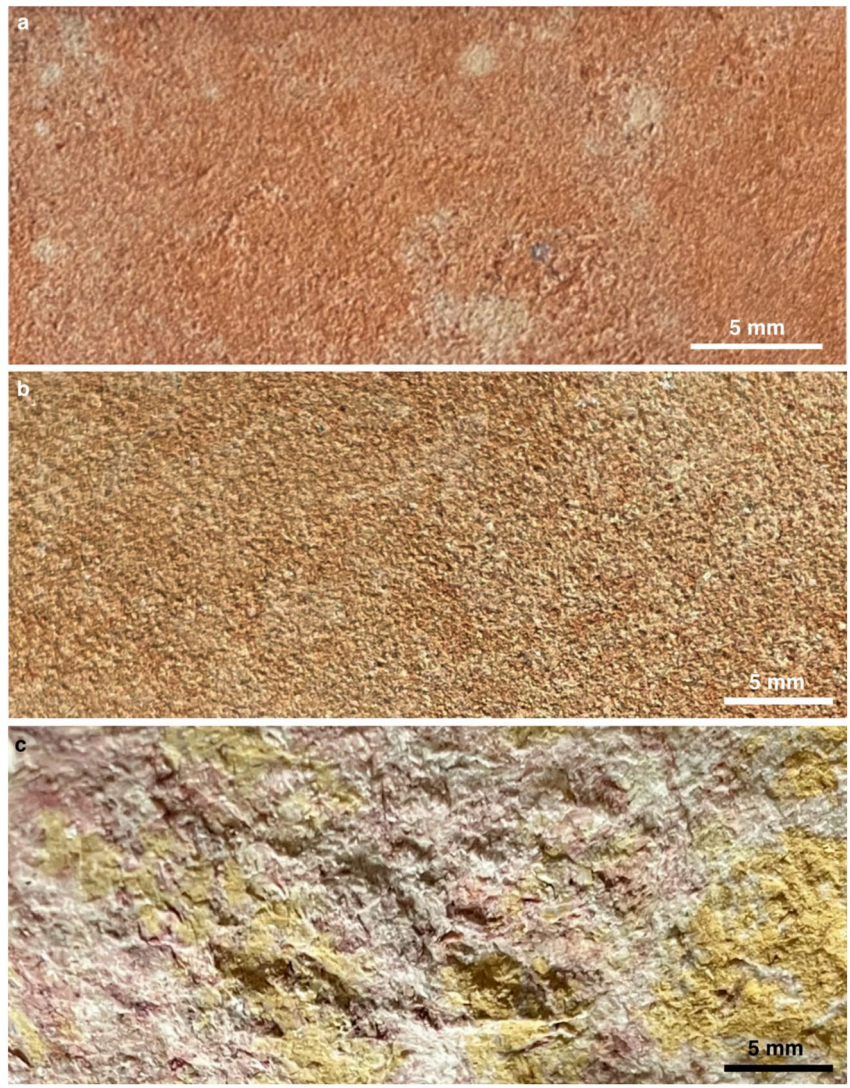

Figure 15. Possible terrestrial analogs. (a) Permian Ninnescah Shale fine sandstone from 821.4 m depth in the Amoco Rebecca K. Bound core, Greeley County, Kansas. (b) Triassic Dockum Group fine sandstone from 491 m depth in the Amoco Rebecca K. Bound core, Greeley County, Kansas. (c) modern siltstone from 14.9 m depth in LA2-09 core from acid-saline-ephemeral Lake Aerodrome, Cowan Basin, Western Australia. All three images show bedding plane-parallel views in rock cores without a polished surface; top two rocks (a) and (b) were cut using a rock saw and likely display surface texture similar to abrasion patches Berry Hollow and Uganik Island imaged in situ by Perseverance Rover; bottom rock (c) is the view of natural breakage plane (parallel to bedding). Note pink and tan mottling and cream-colored isopachous intergranular cement around individual grains. All three terrestrial rocks have mineral assemblages similar to the Hogwallow Flats and Yori Pass rocks, including siliciclastic and clastic sulfate grains, and several generations of sulfate and Fe-oxide cement. All three photos were taken in natural light.

were blown into these environments. This strongly suggests that chemical precipitates such as sulfate minerals are excellent repositories for organic materials. The suite of organic materials in salt minerals most typically represents a mixture of both extremophile species indigenous to the parent water as well as "migrant" organic materials that have been transported into the parent water (Benison, Bosak, et al., 2023; Benison, Hallsworth, et al., 2023).

Another possible terrestrial analog is the Lake St. Martin impact structure in Manitoba, Canada, a ~40 km complex crater with a central uplift (Leybourne et al., 2007; McCabe & Bannatyne, 1970; Reimold et al., 1990). This impact structure is similar in size to the Jezero crater. Crater deposits above the impact melt sheet include red beds, which are roughly laminated unsorted deposits of gypsum-cemented clasts of carbonates, Precambrian granitic rocks, and impact melt as well as red-orange-yellow gypsum clasts. These are overlaid by tens of meters

thick deposits of anhydrite/gypsum/glauberite evaporites. The red beds are presumed to have been deposited within the impact structure from an ocean-connected salina located west of the crater (Leybourne et al., 2007). Emplacement was likely rapid as clasts up to ~25 cm are present. Extant endolithic communities have been recognized in and on gypsum cobbles (Cloutis et al., 2021; Rhind et al., 2014).

Although morphological biosignatures in the form of microbial textures, such as stromatolites, have been observed in many bedded gypsums of various ages in the rock record (i.e., Allwood et al., 2013; Bradford, 2023; Bradford et al., 2022; Dela Pierre et al., 2014), cells and biotic organic compounds within salt crystals have been the subjects of fewer studies. Most cells and organic matter in salt minerals have been identified mainly in bottom-growth and cumulate crystals, those that precipitate directly from surface saline water bodies, such as lakes and lagoons (i.e., Benison & Karmanocky, 2014; Conner & Benison, 2013; Lowenstein et al., 2011). However, microorganisms have also been found in fluid inclusions in reworked gypsum crystals. Modern gypsum from White Sands National Park dunes, modern gypsum from sandflats and dunes adjacent to acid saline lakes in Western Australia and Chile, and unaltered Triassic gypsum grains in eolian sandstones from the Chugwater Group of Wyoming all contain biosignatures (Benison, 2019a; Benison et al., 2016). Less is known about microorganisms in sulfate cement, only because few studies, to date, have examined them for biosignatures. However, the presence of microbial life in groundwater that precipitate diagenetic sulfates suggests the strong possibility of biosignatures in sulfate cement (i.e., Zaikova et al., 2018).

6.2. What Types of Diagenetic Fluids Affected the Hogwallow Flats Member and Uganik Island Outcrops?

The fluids that precipitated multiple generations of cement in these rocks were likely shallow saline groundwater. "Groundwater" here is used to indicate any liquids below a planetary surface located in pore spaces between sediment grains or in rocks. Groundwater can exist in the vadose zone as they travel upward or downward, or they can be part of the phreatic zone (below the water table). On Earth, they can be millimeters to kilometers below the subaerial sediment/rock–air interface. Groundwater on Earth have various sources, including meteoric precipitation and hydrothermal fluids. We detected no close-contact, compacted, or deformed grains, indicating that these rocks were likely never deeply buried. All diagenetic features described are capable of forming from shallow saline groundwater on Earth. So, although we cannot determine the source of the groundwater at this time, we can suggest that they were relatively shallow.

Although it is difficult to accurately match some of the minerals and colors of the diagenetic features in Berry Hollow and Uganik Island due to the generally small grain and crystal sizes and similarities in spectral signatures of similar sulfate minerals, we can make some educated guesses. The light-colored parts of the rocks are likely Ca-sulfate and Fe(II)-Mg-sulfate minerals. The reds, oranges, and yellows may be hematite, jarosite, and goethite. Confirmation of anhydrite for the veins has been made (Hurowitz et al., 2023; Lopez-Reyes et al., 2023). From these observations, we can reason that diagenetic fluids were sulfate-rich, some with relatively high amounts of dissolved Ca, Fe, and Mg as well.

Sulfate-rich groundwater can exist at a wide range of pH values. However, those that exist concurrently with Fe-oxides are suggestive of acid saline waters. Jarosite and copiapite are hallmarks of acids because they are known only on Earth to have formed from low pH (generally less than pH 3) waters. Phyllosilicates can be either products of aqueous alteration or direct precipitates from acid or alkaline brines. The phyllosilicates detected in these abrasion patches do not correspond in any obvious way to any diagenetic feature observed; they may exist as the dark grains. In the case that the phyllosilicates are clastic grains, they may not be indicators of the depositional or diagenetic environment of these rocks. Possible detections of chlorides and carbonates in the abrasion patches should also be considered, even though this first attempt at petrographic descriptions did note any obvious chloride or carbonate features. Chlorides, such as halite, indicate high salinity but form at any pH. Chlorides can form as chemical sediments in surface waters, such as lakes. They can also precipitate in various forms, including intergranular cement, displacive cement, vein- and vug-filling cement, and replacement phases of other minerals, including sulfates. In contrast, carbonates would indicate a moderate--high pH fluid, but only if the carbonates are in the form of depositional grains and/or unaltered cement. Carbonates are also known to form as late-stage replacements of Ca-sulfate minerals. Therefore, our preliminary interpretation is that these Martian groundwater that existed in the Jezero fan were likely acid saline groundwater, at least at some point in their history.

6.3. Potential Habitability of Hogwallow Flats Member and Yori Pass Member

Because sulfate minerals precipitate from surface waters and groundwater, we suggest that the depositional and diagenetic sulfates could have had habitable sources. The sand and silt grains in Hogwallow Flats and Yori Pass members are the records of deposition in these locations. The clastic nature of the rock indicates that these grains moved from elsewhere. In contrast, to confirm a saline surface water body at the time of deposition, one would need to observe beds of bottom-growth and/or cumulate crystals, which we did not observe here. However, sulfate sand and silt grains must have precipitated from sulfate-rich saline water. That water may have been a surface water or a groundwater, although the former is more likely because cumulate or bottom-growth crystals are typically larger than sulfate cement and other diagenetic sulfate phases. In addition, cumulate and bottom-growth crystals that formed in saline lakes may have had better opportunity to be eroded and reworked at the planetary surface, especially if the lakes had been ephemeral (see Figure 14a). Therefore, we propose that the sulfate mineral grains were formed as crystals in saline lake waters elsewhere and then moved as clasts to the depositional environments of Hogwallow Flats and Yori Pass.

We cannot directly assess habitability for the depositional environment of Hogwallow Flats and Yori Pass members because clastic grains, if deposited in a subaqueous environment, give no clues about surface water chemistry. In addition, we cannot rule out an eolian environment, which would also not provide any indicators of habitability during deposition. We have not yet identified any sedimentary textures or sedimentary structures that favor subaqueous or subaerial deposition. However, the sulfate mineralogy of some of the grains strongly suggests that those grains precipitated as bottom-growth or cumulate crystals in a saline subaqueous environment (such as a saline lake or spring) upstream or laterally adjacent to the Hogwallow Flats and Yori Pass locations. That subaqueous source environment may have desiccated, which would have subaerially exposed any sulfate bottom-growth and/or cumulate crystals and made them vulnerable to erosion and transportation by winds or later surface waters. Chemical sediments such as sulfates precipitated in lakes or springs can be re-worked and re-deposited in various environments, including freshwater lakes, saline lakes, rivers, deltas, sandflats, and dunes. Thus, any sulfate grains may be remnants of habitable environments elsewhere that can be found in a multitude of depositional environments (see Figure 14a). Thus, any sulfate grains may be remnants of habitable environments elsewhere that can be found in a multitude of depositional settings (see Figure 14a). The sulfate sand and silt grains may contain fluid and solid inclusions in their interiors that may contain parent saline lake or spring waters, atmosphere and other gases, cells, and organic compounds. In this case, analyses of these sulfate sand and silt grains in labs on Earth may reveal environmental proxies of the source saline surface water environment, including potential biosignatures.

The sulfate cement in Hogwallow Flats and Yori Pass rocks all formed in situ from saline groundwater. Saline groundwater are known on Earth to host organic materials, including microorganisms and organic compounds. The multiple diagenetic phases of sulfates suggest that multiple waters flowed through these rocks at different times in the history of the rocks, providing multiple possible times in which the shallow subsurface setting may have been habitable. Any biosignatures present may have been entrapped in sulfate cement as they formed.

Water chemistry can be evaluated for habitability potential. Hogwallow Flats and Yori Pass rocks contain several minerals that are indicators of water chemistry; however, they appear to suggest changing water composition over time. The clastic grains deposited at these two sites do not provide any evidence of surface water characteristics at those locations. We cannot confidently conclude that the depositional environments at Hogwallow Flats and Yori Pass for these grains were subaqueous, and even if it was subaqueous, we do not know the water depth, salinity, pH, or composition. Any Ca-sulfate grains would have been sourced from an environment elsewhere that once may have had a surface water enriched in calcium and sulfate. As for the various diagenetic sulfate minerals, a refined paragenetic sequence may help understand groundwater chemistry over time. For example, if jarosite/copiatite co-precipitated with Ca- or Mg-Fe-sulfates, this would indicate that groundwater was acidic, as jarosite and copiapite precipitate only from acid sulfate brines and acid waters may be enriched in Fe. In contrast, if some Ca-sulfates, including anhydrite, formed at a distinct time different from precipitation time of these acid minerals, they may indicate Ca-SO_4-enriched water, but at any pH.

6.4. What Environmental Indicators May Be Present in the Sulfate Minerals in the Bearwallow, Hazeltop, and Kukaklek Samples?

Sulfate minerals and other saline minerals commonly contain, in their crystal interiors, microsamples of their parent environment that can remain preserved for hundreds of millions of years and indicate detailed information

about their environment of formation (i.e., Benison, 2013; Goldstein, 2001; Lowenstein et al., 2011). Because sulfate minerals precipitate from waters and grow relatively quickly, they tend to entrap fluid inclusions along imperfections in growth bands as they grow (Goldstein & Reynolds, 1994). These fluid inclusions can be up to ~400 μm long. Their orientation along growth bands testifies to their entrapment during the growth of the host mineral; we call these primary fluid inclusions. In contrast, secondary fluid inclusions are situated along planes that cross-cut growth bands and crystal boundaries, indicating that they were formed by later fluids that migrated through a crystal along microfractures (Goldstein & Reynolds, 1994). In addition to water and gases, sulfate minerals can also trap solids as solid inclusions.

Primary fluid inclusions contain a liquid and/or gas (Goldstein & Reynolds, 1994; Roedder, 1984). They may also contain solid minerals in the form of true or accidental "daughter crystals." Fluid inclusions can also contain various organic materials, including cells of microorganisms and liquid, solid, and/or gas organic compounds. Some growth bands in sulfate minerals also host solid inclusions associated with primary fluid inclusions. These are mineral or organic solids trapped within the host sulfate crystal (see next section for description of organic materials in fluid inclusions). Petrography is the key for distinguishing primary fluid inclusions and solid inclusions from any secondary inclusions. In addition, petrographic observations of phases within fluid inclusions are an important foundational step to guide further analyses aimed at identifying those phases.

Fluid inclusion analyses can be used to determine water temperature at the time of crystal growth, pressure of entrapment, liquid composition (including salinity, pH, and major ions), and gas and solid compositions (Goldstein & Reynolds, 1994). There is a large range of studies that can be conducted on fluid inclusions (Benison, 2013). Some are non-destructive and are performed in situ on individual inclusions, such as the microthermometry techniques known as homogenization runs, which determine the temperature of formation, and freezing-melting runs, which analyze for total salinity and major ion content (i.e., Benison & Goldstein, 1999; Benison & Lowenstein, 1997; Davis et al., 1990; Karmanocky & Benison, 2016; Roberts & Spencer, 1995). Laser micro-Raman spectroscopy of individual phases in fluid inclusions is an in situ, non-destructive technique that has been used to measure pH and compositions of parent waters, as well as identify minerals and organic compounds within fluid inclusions (Benison et al., 1998; Jagniecki & Benison, 2010; Winters et al., 2013). UV-vis petrography can detect fluorescent response of organic materials in fluid inclusions or as solid inclusions (Conner & Benison, 2013). Other analyses performed in situ on individual inclusions include techniques such as ESEM-EDS and LA-MS, which have been used to interpret past seawater and lake water compositions (i.e., Brennan et al., 2004). Laser pyrolysis and time-of-flight secondary ion mass spectrometry have also been used to study organic biomarkers in fluid inclusions (Siljeström et al., 2010, 2013, 2022; Zhang et al., 2012). In addition, there are many analytical techniques that can be performed destructively by crushing host crystals and extracting inclusion fluids, gases, and organic material. Examples include the measurement of oxygen content in entrapped Proterozoic atmosphere in fluid inclusions in halite (Blamey et al., 2016) and identification of archaeal, bacterial, and algal species in fluid inclusions in halite (i.e., Norton & Grant, 1988).

The reworked sulfate grains and diagentic sulfate crystals in the Bearwallow, Hazeltop, and Kukaklek samples have the potential to contain fluid and solid inclusions. These fluid inclusions could be a treasure trove of information about both biosignatures and past environmental conditions of the Jezero crater fan front. Fluid and/or solid inclusions in reworked sulfate grains would provide environmental information about surface water environments that existed prior to, or laterally adjacent to the depositional sites of the middle Shenandoah formation. Possible data could include air composition, water temperature, water salinity, composition, pH, and microorganisms and organic compounds. Additionally, fluid inclusions in the diagenetic sulfate minerals found as intergranular cement, possible overgrowth cement, and vein and vug cements may record data about past groundwater temperatures, salinities, compositions, pHs, and microorganisms and organic compounds.

6.5. Types of Biosignature Preservation Possible in Sulfate Clastic Grains and Diagenetic Sulfate Cements

Biosignatures have been documented in the interiors of crystals of gypsum, anhydrite, and mirabilite on Earth (Figure 16). Microorganisms and organic compounds can be entrapped as solids and within fluid inclusions as sulfate minerals grow quickly. Cells of archaea, bacteria, and algae as well as fungi, pollen, and insects have been found in sulfate minerals (i.e., Benison & Karmanocky, 2014; Gill et al., 2023). In addition, organic compounds such as beta-carotene and glycerine have also been detected (Benison & Karmanocky, 2014; Gill et al., 2023).

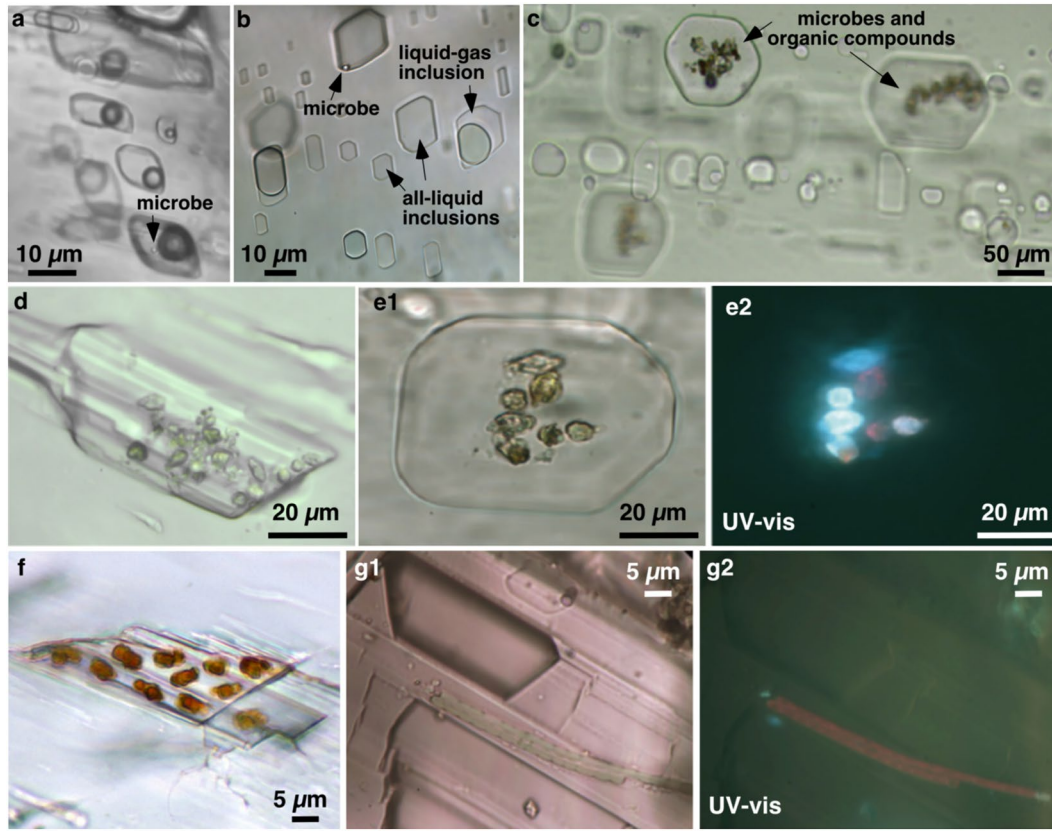

Figure 16. Microbes in primary fluid inclusions and solid inclusions in terrestrial sulfate minerals. (a) Liquid-gas fluid inclusions in wind-deposited gypsum clast from Salar Gorbea, Chile. Arrow points to prokaryotic cocci. Modified from Benison (2019a). (b) All-liquid and liquid-gas fluid inclusions in White Sands gypsum dune sand. (c) Mirabilite from spring in Great Salt Lake, Utah, USA Modified from Gill et al. (2023). (d) Yellow algae and clear prokaryotes in primary fluid inclusion in bottom-growth gypsum crystals, Lake Aerodrome, Cowan Basin, Western Australia. Modified from Benison (2019a). (e1) Transmitted light and (e2) paired UV-vis (330 and 385 nm) light views of microorganisms in primary fluid inclusion in mirabilite from Great Salt Lake, Utah, USA Modified from Gill et al. (2023). (f) Algae, partially coated in beta-carotene, in wind-deposited gypsum crystal from Salar Ignorado, Chile. Modified from Benison and Karmanocky (2014). (g1) Transmitted light and (g2) UV-vis (330 and 385 nm) light views of suspect green alga and prokaryotes trapped as solid inclusions in growth band with primary fluid inclusions in gypsum dune sand adjacent to Lake Aerodrome, Cowan Basin, Western Australia.

When trapped within a fluid inclusion, cells and organic compounds are in a microhabitat that may provide a host environment for long geological time periods (i.e., Lowenstein et al., 2011; Schreder-Gomes et al., 2022). Regardless of whether biosignatures are trapped as solid inclusions or within fluid inclusions, their location the interior of crystals probably protects them from decay that would otherwise occur on the planetary surface when exposed to atmosphere and radiation.

Relatively few studies have focused on microorganisms and organic compounds within sulfate minerals (i.e., Benison & Karmanocky, 2014; Dela Pierre et al., 2015; Gill et al., 2023). Those studies are dominated by analyses of either natural or laboratory-grown chemical sediments, such as bottom-growth or cumulate crystals (see Figure 14). In the literature, there are only a few mentions of biosignatures in reworked gypsum clasts (Benison & Karmanocky, 2014; Karmanocky & Benison, 2016). Little is known about the potential of biosignatures in sulfate cement. However, early, shallow acid saline groundwater surveyed in Western Australia contain a diverse microbial population (i.e., Zaikova et al., 2018). These same groundwater precipitate sulfate intergranular cement, overgrowth cement, and displacive crystals. Therefore, although untested to date, there is a possibility that the sulfate cement in the Hogwallow Flats and Yori Pass rocks may contain organic materials.

Of the two main forms of sulfate in these Martian rocks, the reworked sulfate clasts likely have a higher potential for hosting biosignatures. Because chemical sediments (those saline mineral crystals that precipitate from surface

saline waters) grow quickly, they contain abundant imperfections on their crystal faces as they grow; these imperfections become microscopic pockets of parent liquid that are covered over with the host crystal as it continues to grow. In contrast, groundwater precipitate minerals at a slower pace; thus, cement, in general, tend to have fewer entrapped primary fluid inclusions that can serve as host microhabitats for microorganisms and organic compounds. Although we propose that any of the sulfates at Hogwallow Flats and Yori Pass have the potential to have trapped and preserved biosignatures, if they were present, the reworked sulfate clasts likely have a higher potential for biosignatures than do the sulfate cement.

Another way to preserve biosignatures over long geologic time periods is within Fe-oxide concretions (see Figure 6.2 in Farmer et al., 2009). Sulfate and chloride minerals that contain biosignatures can be incorporated within concretions when Fe-oxide cement grow around the sulfate grains or crystals. The Fe-oxide then provides further protection from possible dissolution from later dilute waters and radiation.

The rocks of Hogwallow Flats and Yori Pass have the potential to contain biosignatures. If the sulfates have organic materials as solid inclusions or within fluid inclusions, they would not be easily detected by in situ analyses performed by the Perseverance rover. In terrestrial sulfate minerals, the requirements to detect these cells and organic compounds include transmitted microscopy and/or UV-vis fluorescence microscopy at the 400–2,000× magnification range with long-working distance microscope objectives, as well as laser Raman spectrometry at similar magnification and focus. The total amount of organic material in such cases is low, and the high resolution of analytical instruments focused into crystal interiors is needed (i.e., Gill et al., 2023; Lowenstein et al., 2011; Schreder-Gomes et al., 2022). However, when compared with known preservation in terrestrial analog sulfate minerals, we suggest that the Hogwallow Flats and Yori Pass sulfate minerals have the potential to host biosignatures.

7. Conclusions

The Bearwallow, Hazeltop, and Kukaklek rock cores sampled at Hogwallow Flats and Yori Pass contain a record of deposition and a series of diagenetic fluid events. Sulfate cement crystals suggest saline groundwater. Depositional and diagenetic sulfates here have the potential to contain fluid inclusions that may yield environmental conditions such as past water temperatures, salinities, compositions, and pH. In addition, such sulfates are known to have preserved biosignatures in the geologic record of Earth. Future analyses of these sulfates in laboratory facilities on Earth may provide answers to questions about past Martian environments, habitability, and life.

Data Availability Statement

The data in this publication are from the Mastcam-Z, PIXL, and Watson instruments of the Mars 2020 Perseverance rover. These data are also available in the NASA PDS archive, including Mastcam-Z (Bell & Maki, 2021), PIXL (Allwood & Hurowitz, 2021), and Watson/SHERLOC (Beagle, 2021). The images shown in Figures 2, 5–7, 8a, 10a[5–7], and 11 can be found in Initial Reports M2020-509-14 Hazeltop. M2020-516-15 Bearwallow, and M2020-623-19 Kukaklek (Farley & Stack, 2023, https://doi.org/10.17189/49zd-2k55, https://pds-geosciences.wustl.edu/m2020/urn-nasa-pds-mars2020_sample_dossier/initial_reports_volume2.pdf) in the NASA Planetary Data System archive. Images appearing in Figures 8b and 9 are cropped close-up views of Figure 8a. Images appearing as Figure b–e are cropped close-up views of Figure 10a.

Acknowledgments
We thank the entire Mars 2020 science, engineering, and leadership team. K. C. Benison and K. K. Gill acknowledge funding from National Aeronautics and Space Administration Grant 80NSSC20K0235 to K.C.B. T. Bosak is supported by NASA Grant 80NSSC20K0234 and the Simons Foundation Collaboration on the Origins of Life #327126. E. A. Cloutis acknowledges funding from the Canadian Space Agency (Grants 15FASTA05 and 22EXPCOI4), the Natural Sciences and Engineering Research Council of Canada (Grants RGPIN-2015-0452, RTI-2020-00157, and RGPIN-2023-03413), the Canada Foundation for Innovation and Research Manitoba (Grants CFI1504 and CFI-2450). F. Fornaro was funded through the ASI/INAF Agreement n. 2023-3-HH. C. D. K. Herd and N. Randazzo acknowledge funding from the Canadian Space Agency (20EXPMARS), and the Natural Sciences and Engineering Research Council of Canada (Grant RGPIN-2018-04902 to C.D.K.H.). J. M. Madariaga and J. M. Frias acknowledge funding from the Spanish Agency for Research AEI/MCIN/FEDER Grant PID2022-142750OB-I00. M. Nachon was funded by NASA M2020 Participating Scientist Grant 80NSSC21K0329. S. Sharma, K. Hand, and K. Uckert acknowledge funding from the National Aeronautics and Space Administration (80NM0018D0004) to support research that was carried out at the Jet Propulsion Laboratory, California Institute of Technology. S. Siljeström acknowledges funding from the Swedish National Space Agency, contract 2021-00092. A. Williams acknowledges funding from NASA 80NSSC21K0332. We thank editor Bradley Thomson, guest associate editor Gwénaël Caravaca, and anonymo reviewers for constructive comments.

References

Allwood, A. C., Burch, I. W., Rouchy, J. M., & Coleman, M. (2013). Morphological biosignatures in gypsum. Diverse formation processes of Messinian (~6.0 Ma) gypsum stromatolites. *Astrobiology*, *13*, 870–885. https://doi.org/10.1089/ast.2013.1021

Allwood, A. C., & Hurowitz, J. A. (2021). *Mars 2020 PIXL raw and processed data Bundle*. NASA Planetary Data System. https://doi.org/10.17189/1522645

Allwood, A. C., Wade, L. A., Foote, M. C., Elam, W. T., Hurowitz, J. A., Battel, S., et al. (2020). PIXL: Planetary instrument for X-ray lithochemistry. *Space Science Reviews*, *216*, 134. https://doi.org/10.1007/s11214-021-00801-2

Beagle, L. (2021). *Mars 2020 SHERLOC Bundle*. NASA Planetary Data System. https://doi.org/10.17189/1522643

Bell, J. F., & Maki, J. N. (2021). *Mars 2020 mast camera zoom Bundle, from Arizona state University Mastcam-Z instrument team, calibrated products*. NASA Planetary Data System. https://doi.org/10.17189/Q3TS-C749

Bell, J. F., III, Maki, J. N., Mehall, G. L., Ravine, M. A., Caplinger, M. A., Bailey, Z. J., et al. (2021). The Mars 2020 Perseverance rover mast camera zoom (Mastcam-Z) multispectral, stereoscopic imaging investigation. *Space Science Reviews*, *217*(1), 24. https://doi.org/10.1007/s11214-020-00755-x

Benison, K. C. (2013). Acid saline fluid inclusions: Examples from modern and Permian extreme lake systems. *Geofluids*, *13*(4), 579–593. https://doi.org/10.1111/gfl.12053

Benison, K. C. (2017). Gypsum gravel devils in Chile: Movement of largest natural gains by wind? *Geology*, *45*(5), 423–426. https://doi.org/10.1130/G38901.1

Benison, K. C. (2019a). How to search for life in Martian chemical sediments and their fluid and solid inclusions using petrographic and spectroscopic methods. *Frontiers in Environmental Science*, *7*, 108. https://doi.org/10.3389/fenvs.2019.00108

Benison, K. C. (2019b). The physical and chemical sedimentology of two high-altitude acid salars in Chile: Sedimentary processes in an extreme environment. *Journal of Sedimentary Research*, *89*(2), 147–167. https://doi.org/10.2110/jsr.2019.9

Benison, K. C., & Bowen, B. B. (2013). Extreme sulfur-cycling in acid brine lake environments of Western Australia. *Chemical Geology*, *351*, 154–167. https://doi.org/10.1016/j.chemgeo.2013.05.018

Benison, K. C., Bowen, B. B., Oboh-Ikuenobe, F. E., Jagniecki, E. A., LaClair, D. A., Story, S. L., et al. (2007). Sedimentology of acid saline lakes in southern Western Australia: Newly described processes and products of an extreme environment. *Journal of Sedimentary Research*, *77*(5), 366–388. https://doi.org/10.2110/jsr.2007.038

Benison, K. C., Bosak, T., Clark, B. C., Czaja, A. D., Fornaro, T., Gill, K. K., et al. (2023). Biosignature potential and possible environmental indicators of sulfate-rich rocks from Hogwallow Flats and Yori Pass, Jezero crater delta front, Mars. In *Proceedings of the 54th lunar and planetary science conference (LPSC), Lunar and planetary Institute, abstract 2570*.

Benison, K. C., Goldstein, R. H., Wopenka, B., Burruss, R. C., & Pasteris, J. D. (1998). Extremely acid Permian lakes and ground waters in North America. *Nature*, *392*(6679), 911–914. https://doi.org/10.1038/31917

Benison, K. C., & Goldstein, R. H. (1999). Permian paleoclimate data from fluid inclusions in halite. *Chemical Geology*, *154*(1–4), 113–132. https://doi.org/10.1016/S0009-2541(98)00127-2

Benison, K. C., Hallsworth, J. E., Zalar, P., Glavina, M., Gibson, M. E., Gill, K. K., et al. (2023). How can fungi in extreme acid lakes and their salts inform us about possible life on Mars? In *First international conference on extremophilic fungi (Fun-Ex), International union of Biochemistry and molecular biology, Ljubljana, Slovenia*.

Benison, K. C., & Karmanocky, F. J., III. (2014). Could microorganisms be preserved in Mars gypsum? Insights from terrestrial examples. *Geology*, *42*(7), 615–618. https://doi.org/10.1130/G35542.1

Benison, K. C., Karmanocky, F. J., III, & Knapp, J. P. (2016). Can fluid inclusions in eolian gypsum be used to interpret past lake conditions, chemistry, and microbiology? In *Abstracts with program, Geological Society of America annual meeting abstracts with programs, Denver, Colorado* (Vol. 48, p. 7). https://doi.org/10.1130/abs/2016AM-283488

Benison, K. C., & Lowenstein, T. K. (1997). Carbonate-hosted mineralization of the lower Ordovician Ogdensburg formation: Evidence for a Paleozoic thermal anomaly in the St. Lawrence-Ottawa lowlands of New York and Ontario. In I. P. Montanez, J. M. Gregg, & K. L. Shelton (Eds.), *Basin-wide diagenetic Patterns: Integrated Petrologic, geochemical, and hydrologic considerations*. SEPM Special Publication. https://doi.org/10.2110/pec.97.57.0207

Benison, K. C., O'Neill, W., Blain, D., & Hallsworth, J. E. (2021). Water activities of acid brine lakes approach the limit for life. *Astrobiology*, *21*(6), 729–740. https://doi.org/10.1089/AST.2020.2334

Blamey, N. J., Brand, U., Parnell, J., Spear, N., Lécuyer, C., Benison, K., et al. (2016). Paradigm shift in determining neoproterozoic atmospheric oxygen. *Geology*, *44*(8), 651–654. https://doi.org/10.1130/G37937.1

Bosak, T., Shuster, D. L., Scheller, E., Siljestrom, S., Zawaski, M., Mandon, L., et al. (2024). Astrobiological potential of samples acquired by the Perseverance rover at the sedimentary fan front in Jezero Crater, Mars. *Journal of Geophysical Research: Planets*.

Bradford, M. Y. (2023). Continental saline environments interpreted from bedded gypsum of the Triassic red Peak formation (Chugwater Group), northcentral Wyoming (2023). In *Graduate theses, dissertations, and problem Reports 11988*. West Virginia University. Retrieved from https://researchrepository.wvu.edu/etd/11988

Bradford, M. Y., Benison, K. C., Knapp, J. P., & Petras, B. (2022). Gypsum textural records of continental saline environments from the Triassic Red Peak Formation, Wyoming. In *Geological Society of America abstracts with programs, Denver, Colorado* (Vol. 54, p. 5). https://doi.org/10.1130/abs/2022AM-380236

Brennan, S. T., Lowenstein, T. K., & Horita, J. (2004). Seawater chemistry and the advent of biocalcification. *Geology*, *32*(6), 473–476. https://doi.org/10.1130/G20251.1

Broz, A. P., Horgan, B. H., Kalucha, H., Garczynski, B., Haber, J., Hurowitz, J., et al. (2023). Diagenetic alteration of Hogwallow flats, Jezero crater, Mars. In *Proceedings of the 54th lunar and planetary science conference (LPSC), lunar and planetary Institute, abstract 1845*.

Cloutis, E., Stromberg, J., Applin, D., Connell, S., Kubanek, K., Kuik, J., et al. (2021). The Lake St. Martin impact structure (Manitoba, Canada): A simulated rover exploration of a sulfate-bearing impact crater. *Planetary and Space Science*, *208*, 105336. https://doi.org/10.1016/j.pss.2021.105336

Conner, A. J., & Benison, K. C. (2013). Acidophilic halophilic microorganisms in fluid inclusions in halite from Lake Magic, Western Australia. *Astrobiology*, *9*, 850–860. https://doi.org/10.1089/ast.2012.0956

Davis, D. W., Lowenstein, T. K., & Spencer, R. J. (1990). Melting behavior of fluid inclusions in laboratory-grown halite crystals in the systems $NaCl{\cdot}H_2O$, $NaCl{\cdot}KCl{\cdot}H_2O$, $NaCl{\cdot}MgCl_2{\cdot}H_2O$, and $NaCl{\cdot}CaCl_2{\cdot}H2O$. *Geochimica et Cosmochimica Acta*, *54*(3), 591–601. https://doi.org/10.1016/0016-7037(90)90355-O

Davis-Belmar, C. S., Pinto, E., Demergasso, C., & Rautenbach, G. (2013). Proteo and Actinobacteria diversity at a sulfide, salt and acid-rich lake in the north of Chile. *Advanced Materials Research*, *825*, 37–41. https://doi.org/10.4028/www.scientific.net/amr.825.37

Dehouck, E., Forni, O., Quantin-Nataf, C., Beck, P., Mangold, N., Royer, C., et al. (2023). Overview of the bedrock geochemistry and mineralogy observed by SuperCam during perseverance's delta front campaign. In *Proceedings of the 54th lunar and planetary science conference (LPSC), lunar and planetary Institute, abstract 2862*.

Dela Pierre, F., Clari, P., Natalicchio, M., Ferrando, S., Giustetto, R., Lozar, F., et al. (2014). Flocculent layers and bacterial mats in the mudstone interbeds of the Primary Lower Gypsum unit (Tertiary Piedmont basin, NW Italy): Archives of palaeoenvironmental changes during the Messinian salinity crisis. *Marine Geology*, *355*, 71–87. https://doi.org/10.1016/j.margeo.2014.05.010

Dela Pierre, F., Natalicchio, M., Ferrando, S., Giustetto, R., Birgel, D., Carnevale, G., et al. (2015). Are the large filamentous microfossils preserved in Messinian gypsum colorless sulfide-oxidizing bacteria? *Geology*, *43*(10), 855–858. https://doi.org/10.1130/G37018.1

Escudero, L., Oetiker, N., Gallardo, K., Tebes-Cayo, C., Guajardo, M., Nunez, C., et al. (2018). A thiotrophic microbial community in an acidic brine lake in Northern Chile. *Antonie van Leeuwenhoek*, *111*(8), 1403–1419. https://doi.org/10.1007/s10482-018-1087-8

Farley, K. A., & Stack, K. M. (2023). *Mars 2020 initial Reports, volume 2: Delta front campaign, NASA technical report*. NASA Planetary Data System. https://doi.org/10.17189/49zd-2k55.232

Farley, K. A., Williford, K. H., Stack, K. M., Bhartia, R., Chen, A., de la Torre, M., et al. (2020). Mars 2020 mission overview. *Space Science Reviews*, *216*(8), 1–41. https://doi.org/10.1007/s11214-020-00762-y

Farmer, J. D., Bell, J. F., III, Benison, K. C., Boynton, W. V., Cady, S. L., Ferris, F. G., et al. (2009). *Assessment of planetary protection requirements for Mars sample return missions* (p. 80). Space Studies Board, National Research Council, National Academy Press.

Gill, K. K., Jagniecki, E. A., Benison, K. C., & Gibson, M. E. (2023). A Mars-analog sulfate mineral, mirabilite, preserves biosignatures. *Geology*, *51*(9), 818–822. https://doi.org/10.1130/G51256.1

Goldstein, R. H. (2001). Clues from fluid inclusions. *Science*, *294*(5544), 1009–1011. https://doi.org/10.1126/science.1066322

Goldstein, R. H., & Reynolds, T. J. (1994). *Systematics of fluid inclusions in diagenetic minerals* (Vol. 31). SEPM Society for Sedimentary Geology.

Herd, C. D. K., Bosak, T., Farley, K. A., Stack, K. M., Benison, K. C., Cohen, B. A., et al. (2023). Sampling by the NASA Perseverance rover for Mars sample return. In *Proceedings of the 54th lunar and planetary science conference (LPSC), lunar and planetary Institute, abstract 2185*.

Hollis, J. R., Sharma, S., Abbey, W., Bhartia, R., Beegle, L., Fries, M., et al. (2023). A deep ultraviolet Raman and fluorescence spectral library of 51 organic compounds for the SHERLOC instrument onboard Mars 2020. *Astrobiology*, *23*, 1–23. https://doi.org/10.1089/ast.2022.0023

Hurowitz, J. A., Tice, M. M., Allwood, A. C., Cable, M. L., Bosak, T., Broz, A., et al. (2023). The Petrogenetic history of the Jezero crater delta front from microscale observations by the Mars 2020 PIXL instrument. In *Proceedings of the 54th lunar and planetary science conference (LPSC), lunar and planetary Institute, abstract 2301*.

Jagniecki, E. A., & Benison, K. C. (2010). Criteria for the recognition of acid-precipitated halite. *Sedimentology*, *57*(1), 273–292. https://doi.org/10.1111/j.1365-3091.2009.01112.x

Johnson, S. S., Chevrette, M. G., Ehlmann, B., & Benison, K. C. (2015). Insights from the metagenome of an acid Salt Lake: The role of biology in an extreme depositional environment. *PLoS One*, *10*(4), e0122869. https://doi.org/10.1371/journal.pone.0122869

Kalucha, H., Broz, A. J., Fischer, W., & Gasda, P. J. (2023). In-situ alteration in sulfate rich units of Jezero crater, Mars. In *Proceedings of the 54th Lunar and Planary Science Conference (LPC), Lunar and Planetary Institute, abstract 1291*.

Karmanocky, F. J., III, & Benison, K. C. (2016). A fluid inclusion record of hydrothermal pulses in acid Salar Ignorado gypsum, northern Chile. *Geofluids*, *16*(3), 490–506. https://doi.org/10.1111/gfl.12171

Langford, R. P. (2003). The Holocene history of the White Sands dune field and influences on eolian deflation and playa lakes. *Quaternary International*, *104*(1), 31–39. https://doi.org/10.1016/S1040-6182(02)00133-7

Leybourne, M. I., Denison, R. E., Cousens, B. L., Bezys, R. K., Gregoire, D. C., Boyle, D. R., & Dobrzanski, E. (2007). Geochemistry, geology, and isotopic (Sr, S, and B) compo-sition of evaporites in the Lake St. Martin impact structure: New constraints on the age of melt rock formation. *Geochemistry, Geophysics, Geosystems*, *8*(3), 22. https://doi.org/10.1029/2006GC001481

Longo, G. M., Piccinni, V., & Longo, S. (2019). Evaluation of $CaSO_4$ micrograins in the context of organic matter delivery: Thermochemistry and atmospheric entry. *International Journal of Astrobiology*, *18*(4), 345–352. https://doi.org/10.1017/S1473550418000204

Lopez-Reyes, G., Nachon, M., Veneranda, M., Beyssac, O., Madariaga, J. M., Manrique, J. A., et al. (2023). Anhydrite detections by Raman spectroscopy with SuperCam at the Jezero delta, Mars. In *Proceedings of the 54th lunar and planetary science conference (LPSC), lunar and planetary Institute, abstract 1721*.

Lowenstein, T. K., Schubert, B. A., & Timofeeff, M. N. (2011). Microbial communities in fluid inclusions and long-term survival in halite. *Geological Society of America Today*, *21*(1), 4–9. https://doi.org/10.1130/GSATG81A.1

Martinez-Frias, J., Amaral, G., & Vázquez, L. (2006). Astrobiological significance of minerals on Mars surface environment. *Reviews in Environmental Science and Biotechnology*, *5*(2–3), 219–231. https://doi.org/10.1007/s11157-006-0008-x

Maurice, S., Wiens, R. C., Bernardi, P., Cais, P., Robinson, S., Nelson, T., et al. (2021). The SuperCam Instrument suite on the Mars 2020 rover: Science objectives and mast-unit description. *Space Science Reviews*, *217*(3), 1–108. https://doi.org/10.1007/s11214-021-00807-w

McCabe, H. R., & Bannatyne, B. B. (1970). Lake St. Martin crypto-explosion crater and geology of the surrounding area. *Geological Survey Manitoba Geological Paper*, *3*(70), 1–69.

Mees, F., Casteñeda, C., Herrero, J., & Van Ranst, E. (2012). The nature and significance of variations in gypsum crystal morphology in dry lake basins. *Journal of Sedimentary Research*, *82*(1), 37–52. https://doi.org/10.2110/jsr.2012.3

Moeller, R. C., Jandura, L., Rosette, K., Robinson, M., Samuels, J., Silverman, M., et al. (2021). The sampling and caching subsystem (SCS) for the scientific exploration of Jezero crater by the Mars 2020 perseverance rover. *Space Science Reviews*, *217*, 1–43. https://doi.org/10.1007/s11214-020-00783-7

Mormile, M. R., Hong, B.-Y., & Benison, K. C. (2009). Molecular analysis of the microbial communities of Mars-analog lakes in Western Australia. *Astrobiology*, *9*(10), 919–930. https://doi.org/10.1089/ast.2008.0293

Mustard, J. F., Adler, M., Allwood, A., Bass, D. S., Beaty, D. W., Bell, J. F., III, et al. (2013). Report of the Mars 2020 science definition team, the Mars exploration program analysis Group (MEPAG) (p. 154). Retrieved from http://mepag.jpl.nasa.gov/reports/MEP/Mars_2020_SDT_Report_Final.pdf

Nachon, M., Lopez-Reyes, G., Meslin, P.-Y., Ollila, A., Mandon, L., Clave, E., et al. (2023). Light-toned veins and material in Jezero crater, Mars, as seen in-situ via NASA's Perseverance rover (Mars 2020 mission): Stratigraphic distribution and compositional results from the SuperCam instrument. In *Proceedings of the 54th lunar and planetary science conference (LPSC), lunar and planetary Institute, abstract 2673*.

Norton, C. F., & Grant, W. D. (1988). Survival of halobacteria within fluid inclusions in salt crystals. *Microbiology*, *134*(5), 1365–1373. https://doi.org/10.1099/00221287-134-5-1365

Núñez, J. I., Johnson, J. R., Rice, M. S., Horgan, B. N., Vaughn, A., Garcyznski, B. J., et al. (2023). Spectral diversity along the delta front in Jezero crater, Mars as seen with Mastcam-Z on the Mars 2020 Perseverance rover. In *Proceedings of the 54th Lunar and planetary science conference (LPSC), lunar and planetary Institute, abstract 3036*.

Phua, Y., Ehlmann, B. L., Mandon, L., Siljeström, S., Razzell Hollis, J., & Bhartia, R. (2023). Characterizing hydration in alteration minerals of Jezero crater geologic units with SHERLOC on Mars-2020. In *Proceedings of the 54th lunar and planetary science conference (LPSC), lunar and planetary Institute, abstract 1392*.

Reimold, W. U., Barr, J. M., Grieve, R. A. F., & Durrheim, R. J. (1990). Geochemistry of the melt and country rocks of the Lake St. Martin impact structure, Manitoba, Canada. *Geochimica et Cosmochimica Acta*, *54*(7), 2093–2111. https://doi.org/10.1016/0016-7037(90)90273-N

Rhind, T., Ronholm, J., Berg, B., Mann, P., Applin, D., Stromberg, J., et al. (2014). Gypsum-hosted endolithic communities of the Kale St. Martin impact structure, Manitoba, Canada: Spectroscopic detectability and implications for Mars. *International Journal of Astrobiology*, *13*(14), 366–377. https://doi.org/10.1017/S1473550414000378

Roberts, S. M., & Spencer, R. J. (1995). Paleotemperatures preserved in fluid inclusions in halite. *Geochimica et Cosmochimica Acta*, *59*(19), 3929–3942. https://doi.org/10.1016/0016-7037(95)00253-V

Roedder, E. (1984). Volume 12: Fluid inclusions. *Reviews in Mineralogy*, *12*, 644.

Roppel, R. D., Abbey, W. J., Asher, S. A., Bhartia, R., Bykov, S. V., Conrad, P., et al. (2023). Investigation of mineralogies during the delta front campaign by SHERLOC. In *Proceedings of the 54th lunar and planetary science conference (LPSC), lunar and planetary Institute, abstract 2761*.

Schreder-Gomes, S. I., Benison, K. C., & Bernau, J. A. (2022). 830 million-year-old microorganisms in primary fluid inclusions in halite. *Geology*, *50*(8), 918–922. https://doi.org/10.1130/G49957.1

Sharma, S., Roppel, R. D., Murphy, A. E., Beegle, L. W., Bhartia, R., Steele, A., et al. (2023). Diverse organic-mineral associations in Jezero crater, Mars. *Nature*, *619*(7971), 724–732. https://doi.org/10.1038/s41586-023-06143-z

Siljeström, S., Lausmaa, J., Sjövall, P., Broman, C., Thiel, V., & Hode, T. (2010). Analysis of hopanes and steranes in single oil-bearing fluid inclusions using time-of-flight secondary ion mass spectrometry (ToF-SIMS). *Geobiology*, *8*(1), 37–44. https://doi.org/10.1111/j.1472-4669.2009.00223.x

Siljeström, S., Volk, H., & George, S. C. (2022). Using ToF-SIMS analyses for analysing individual oil inclusions of different fluorescence colours in a single quartz crystal from the Barrandian (Czech Republic). *Organic Geochemistry*, *164*, 104354. https://doi.org/10.1016/j.orggeochem.2021.104354

Siljeström, S., Volk, H., George, S. C., Lausmaa, J., Sjövall, P., Dutkiewicz, A., & Hode, T. (2013). Analysis of single oil-bearing fluid inclusions in mid-Proterozoic sandstones (Roper Group, Australia). *Geochimica et Cosmochimica Acta*, *122*, 448–463. https://doi.org/10.1016/j.gca.2013.08.010

Simon, J. I., Hickman-Lewis, K., Cohen, B. A., Mayhew, L. E., Shuster, D. L., Debaille, V., et al. (2023). Samples collected from the floor of Jezero crater with the Mars 2020 Perseverance rover. *Journal of Geophysical Research: Planets*, *128*(6), e2022JE007474. https://doi.org/10.1029/2022JE007474

Stack, K. M., Gupta, S., Tebolt, M., Caravaca, G., Ives, L. R. W., Russell, P., et al. (2023). Sedimentology and stratigraphy of the lower delta sequence, Jezero crater, Mars. In *Proceedings of the 54th lunar and planetary science conference (LPSC), lunar and planetary Institute, abstract 1422*.

Tebolt, M., Stack, K. M., Goudge, T. A., Gupta, S., Barnes, R., Caravaca, G., & Brown, A. J. (2023). Characterizing the facies and stratigraphy of the enchanted lake outcrop in Jezero crater, Mars. In *Proceedings of the 54th lunar and planetary science conference (LPSC), lunar and planetary Institute, abstract 2806*.

Wentworth, C. K. (1922). A scale of grade and class terms for clastic sediments. *The Journal of Geology*, *30*(5), 337–424. https://doi.org/10.1086/622910

Wiens, R. C., Maurice, S., Robinson, S. H., Nelson, A. E., Cais, P., Bernardi, P., et al. (2021). The SuperCam instrument suite on the NASA Mars 2020 rover: Body unit and combined system tests. *Space Science Reviews*, *217*, 1–87. https://doi.org/10.1007/s11214-020-00777-5

Williams, A. J., Russell, P. S., Sun, V. Z., Shuster, D., Stack, K. M., Farley, K. A., et al. (2023). Exploring the Jezero delta front: Overview of results from the Mars 2020 perseverance Rover's second science campaign. In *Proceedings of the 54th lunar and planetary science conference (LPSC), lunar and planetary Institute, abstract 1652*.

Williford, K. H., Farley, K. A., Stack, K. M., Allwood, A. C., Beaty, D., Beegle, L. W., et al. (2018). The NASA Mars 2020 rover mission and the search for extraterrestrial life. In *From habitability to life on Mars* (pp. 275–308). Elsevier. https://doi.org/10.1016/B978-0-12-809935-3.00010-4

Winters, Y. D., Lowenstein, T. K., & Timofeeff, M. N. (2013). Identification of carotenoids in ancient salt from death valley, saline valley, and Searles lake, California, using laser Raman spectroscopy. *Astrobiology*, *13*(11), 1065–1080. https://doi.org/10.1089/ast.2012.0952

Zaikova, E., Benison, K. C., Mormile, M. R., & Johnson, S. S. (2018). Microbial communities and their predicted metabolic functions in a desiccating acid salt lake. *Extremophiles*, *22*(3), 367–379. https://doi.org/10.1007/s00792-018-1000-4

Zambito, J. J., IV, Benison, K. C., Foster, T., Soreghan, G. S., Kane, M., & Soreghan, M. J. (2012). Lithostratigraphy of the Permian red beds and evaporites in the Rebecca K. Bounds core, Greeley county. *Kansas: Kansas geological survey open-file report 2012* (Vol. 13, pp. 1–45).

Zhang, Z., Greenwood, P., Zhang, Q., Rao, D., & Shi, W. (2012). Laser ablation GC–MS analysis of oil-bearing fluid inclusions in petroleum reservoir rocks. *Organic Geochemistry*, *43*, 20–25. https://doi.org/10.1016/j.orggeochem.2011.11.005

Zheng, H., McA Powell, C., & Zhoo, H. (2003). Eolian and lacustrine evidence of late Quaternary palaeoenvironmental changes in southwestern Australia. *Global and Planetary Change*, *35*(1–2), 75–92. https://doi.org/10.1016/S0921-8181(02)00137-6